Thermal renders for traditional and historic masonry walls: Comparative study and recommendations for hygric compatibility

Magda Posani [a,b,c,*], Rosário Veiga [b], Vasco Peixoto de Freitas [c]

[a] *ETH Zürich, Institute of Construction and Infrastructure Management (IBI), Chair of Sustainable Construction, Stefano-Franscini-Platz 5, 8093, Zürich, Switzerland*
[b] *Buildings Department, LNEC – National Laboratory for Civil Engineering, Av. Do Brasil 101, 1700-066, Lisboa, Portugal*
[c] *CONSTRUCT (LFC—Laboratory of Building Physics), Faculty of Engineering (FEUP), University of Porto, Rua Doutor Roberto Frias, S/n, 4200-465, Porto, Portugal*

ARTICLE INFO

ABSTRACT

To reach European climate neutrality by 2050, the strategic importance of retrofitting the existing building stock is clear. For this scope, thermal rendering systems have emerged as a very feasible solution for historic and traditionally constructed walls. Nonetheless, a definitive guideline for the selection of suitable solutions for the application in this context is not yet available. This research aims at providing recommendations for the choice of hygric-compatible solutions in an early-stage design, for the context of temperate climates with mild winters. In this study, the massive masonry walls of three historic buildings located in Portugal and Italy are considered. Mono-dimensional hygrothermal simulations are validated against the data measured on-site. Simulations are then used to evaluate the impact of thermal renders on the walls, in comparison to more common insulation materials. Two moisture-related risks are considered: moisture accumulation and reduction of drying. This investigation shows that, for traditional porous walls, retrofitted configurations should be simulated not only under typical operational conditions but also considering a very high initial water content in the wall substrate, when the insulation is applied. Otherwise, moisture-related risks may be overlooked. Recommendations on the choice of thermal rendering systems are provided.

1. Introduction

To reach European climate neutrality by 2050, the strategic importance of a large energy-efficient renovation of the existing building stock is clear [1]. Among the several retrofit solutions that can be adopted, the thermal retrofit of external walls is often considered. Thermal retrofit can lead to improved indoor comfort while reducing operational energy demands [2,3], which is advantageous in both financial and environmental terms [4]. What is more, in the context of historic and traditional urban environments, thermal retrofits are particularly relevant to help maintaining existing buildings in use, thus contributing to conserve these areas as living entities, which is a social and cultural requirement [5]. Thermal retrofits can be performed through post-insulation interventions, with the adoption of thermal insulation on the interior or exterior side of the building envelope. From the building physics point of view, it is normally preferable to apply thermal insulation on the exterior side of walls, because of the lower condensation risks entailed [6]. Furthermore, external insulation offers the chance to reduce rainwater intake in the wall [7], with potential benefits on its thermal performance [8]. On the other hand, the feasibility of the intervention is limited in the context of historic buildings, and it is always excluded for external surfaces holding cultural or tangible values and/or subjected to integral protection constraints [9]. When these circumstances do not occur, external insulation might be installed, especially if the original render is so damaged to require a complete replacement [10]. The intervention is mostly suitable for buildings whose importance is related to the cultural value of "groups of buildings" or landscape [11], and not to the singular construction. In this context, thermal renders are considered as a very feasible solution for the intervention, due to the several benefits they offer [12,13]. Indeed, they can adapt to cracks and irregularities, thus providing for continuous contact between the insulation and the substrate in old walls. Furthermore, they offer great flexibility for the thickness, which can be easily adapted to the dimensional restriction that the intervention may require and it can be adjusted near valuable decorations. In addition, thermal renders require no anchoring points or adhesive layers, as opposed to ETICS (External Thermal Insulation Composite System) solutions [14], which have been extensively used in

* Corresponding author. ETH Zürich, Institute of Construction and Infrastructure Management (IBI), Chair of Sustainable Construction, Stefano-Franscini-Platz 5, 8093, Zürich, Switzerland.
E-mail address: mposani@ethz.ch (M. Posani).

the last decade to insulate new and existing buildings [15]. Furthermore, thermal renders can be applied by mechanical spraying, which facilitates the application [16].

The term thermal render indicates a thermal insulating mortar applied on the exterior side of a wall [17]. A thermal rendering system is an exterior composite insulation solution made of an insulation layer of thermal mortar, covered with one or more coating layers [18]. Finally, the nomenclature thermal mortars is used for mortars with low thermal conductivity, namely below 0.2 W/(m·K) at 10 °C, according to standard EN 998–1:2017 [19].

When applying new renders in historic constructions, physical, mechanical and chemical compatibility should be guaranteed [20–24]. When thermal renders (or other thermal insulation materials) are introduced in this intervention, great concern lies in the physical compatibility, from the hygric point of view [25]. Despite extensive research on this topic, the literature still offers controversial opinions on the correct choice of hygric-compatible thermal insulation solutions, and a definitive guide to good practice is still missing [26]. This problem appears primarily due to the great variety of climates and wall typologies considered, which makes it hardly imaginable to define common solutions and guidelines. Nonetheless, it seems possible to define suitable solutions for specific clusters of situations, namely depending on the type of walls and climates considered [25]. This study focuses on the specific cluster of solid masonry walls of historic and traditionally constructed buildings located in temperate climates with mild winters (temperature rarely going below 0 °C) and on the use of thermal renders. The investigation aims to address the lack of precise guidelines by providing recommendations for the choice of thermal rendering systems in the early stage of the retrofit design. More in detail, this study provides for:

- The moisture-related risks entailed by different types of thermal renders and more commonly adopted insulation materials, such as hydrophobic mineral wool and Expanded Polystyrene;
- Recommendations for the choice of thermal rendering systems in the cluster analyzed, based on the resistance to water vapour diffusion and the capillary water absorption value of the complete insulation solutions.

This paper is organized in the following parts. In Section 2, the methodology adopted in the study is defined. In Section 3 the case studies and the measurements performed on-site are presented. Section 4 is used to introduce the numerical model adopted in the investigation. In the same Section, the input used is explained and the validation of the model is provided. Section 5 outlines the materials and methods adopted for the comparative study on thermal rendering systems and more common insulation solutions. The results are displayed and discussed in Section 6. In Section 7, a synthesis of results is provided. Conclusions are

presented in Section 8.

2. Existing guidelines and previous studies

Despite extensive research on the topic of compatible thermal insulation for traditional and historic solid walls, the literature still offers controversial opinions, and a definitive guide to good practice is still missing [26].

More in detail, several guidelines and some studies report indications for avoiding trapped moisture in historic walls, when using external insulation. The guidelines provided by Historic England on *Energy Efficiency and Historic Buildings* [27] recommend the choice of vapour permeable insulation solutions, and underline that it is generally preferable to progressively increase vapour permeability from the interior of a traditional building to its exterior. Similar recommendations are given in the Guide for improving traditional solid walls in the city of Bath [28]. The guidance notes published by English Heritage [29] and Historic England [30] on *Insulating solid walls* in historic buildings also give analogous indications on vapour permability, while reminding the importance of providing protection from rainwater intake. Both documents preclude the use of closed-cell foam and other plastic-based insulations, as well as protective finishing with high water vapour resistance factors. Despite recommending vapour permeable solutions, all guidelines lack in specificity since they do not set recommended values of water vapour permeability, or quantification of the protection from wind-driven rain, to be used in the choice of insulation systems.

On the contrary, the Cornwall Council Historic Environment Service [31] gives no indication of the recommended properties of thermal insulation, while it underlines the importance of remedying to defects and damp problems in solid walls and allow them to dry out before installation of insulation. Finally, the use of vapour-resistant solutions based on foam panels [32] and closed-cell foams [33] are considered in two US-American guidelines for insulating solid historic walls from the exterior. Nonetheless, the latter guideline underlines that the use of foamed insulation in historic constructions has not been adequately documented yet and that it should be avoided in walls affected by rising damp.

In scientific literature, different opinions can be found too. The European Project EFFESUS [34] developed a thermal mortar with relatively high vapour permeability ($\mu \approx 11.3$) and moderate capillary water absorption value ($A_w \approx 0.4$ kg/(m²h$^{0.5}$)). The mortar was adopted as external insulation, with no additional finishing or rain-protective treatments, on historic walls made of solid bricks and limestones, in the climate of Munich [35]. Layers of 3 cm, 5 cm, and 8 cm were considered and the retrofitted walls were monitored for 6 years. Results show that a vapour permeable thermal render with moderate liquid water absorption coefficient was suitable for keeping acceptable water contents in the walls and avoiding condensation risks. Another study [36] considered an aerogel thermal

render, very vapour permeable ($\mu \approx 4$) and resistant to rainwater intake (A_w not declared, but expected to be low due to the use of organic hydrophobic agent in the mix design [37]). This render was adopted for the external insulation (5–6 cm) of solid stone walls from the 14th century, in Switzerland. Measurements performed on site showed that the vapour permeable and water resistant render was suitable for avoiding moisture accumulation and effective for reducing energy losses through the wall. Numerical simulations were additionally used to show that even in case of moist walls, the vapour permeable nature of the plaster would result in a satisfying drying of the retrofitted wall. On the contrary, an investigation performed in Sweden showed that the use of a vapour and water-proof solution, namely vacuum insulation panels (VIP), improved the overall hygrothermal performance of a historic solid wall. The study underlines that the vapour proof nature of VIP may rise the worrying of entrapped moisture in the wall, but that the study observed no increase of moisture after the adoption of VIP insulation. An attentive read of the article shows that the insulation was applied on a dry wall which was not exposed to moisture threats, such as rising damp. Indeed, the humidity measured inside the wall, before and after the retrofit, stayed below 80%RH. As a consequence, the study indicates that there is no risk of trapped moisture, for the specific scenario considered, which is a wall that does not suffer of unforeseen moisture intake due to damages in the walls, pipes leakage, rising damp or floods.

3. Methodology

The structure of the investigation is synthesized in Fig. 1. The main preparatory steps for the study consist of the choice of three case studies, the measurements performed on-site, and the use of the experimental results for validating numerical simulations. Another fundamental part is the hygrothermal characterization of thermal rendering systems via laboratory testing, which was performed in a previous study by the authors [38]. The data obtained in the aforementioned study are used as input in the numerical simulation tool. Numerical simulations are adopted to study the hygrothermal behaviour of the walls of the three case studies when thermal rendering systems are applied on them. For the sake of comparison, also two more common insulation materials (Expanded Polystyrene and hydrophobic mineral wool [25]) are considered. A parametric study on the hygric properties of one thermal render is also performed.

This study considers thermal insulation solutions with a moderate thickness, namely about 4 cm. This choice is taken because thermal insulation systems with a reduced thickness are normally preferred in the context of historic and traditional urban environments, for the sake of avoiding altering the original geometry and proportion of the buildings, as well as their impact on the landscape. Furthermore, a moderate thickness can be very suitable for the scenario of temperate climates with mild winters.

In this investigation, two moisture-related risks are assessed: moisture accumulation and reduction of drying. The outcomes are collected in a matrix of risk, which is used to compare thermal renders and more common thermal insulation solutions. Results are then used to define recommendations on the choice of thermal rendering systems for minimal moisture-related risks in historic and traditionally constructed massive masonry walls of buildings located in temperate climates with mild winters.

Results are discussed considering the A_w and s_d of the thermal insulation systems, and the indications of DIN 4108-3 [39] and European Assessment Document for ETICS [40] are also accounted for. The first regulation provides recommendations for rain protective stuccos and coatings, considered as layer of a single material applied on the external surface of the wall. It is specific for masonry walls, but it does not refer to multilayer composite insulation systems, such as thermal rendering solutions. The second document is typically used for the
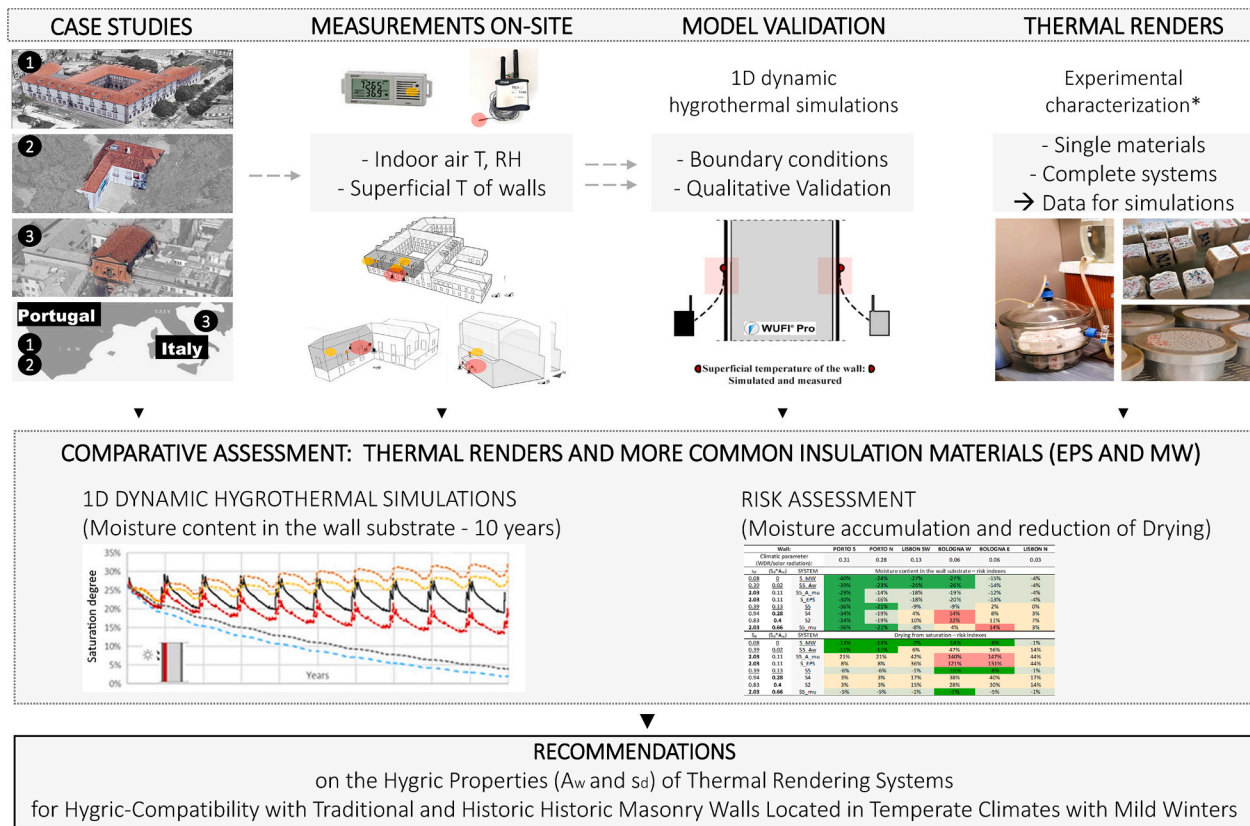

Fig. 1. Methodology adopted in the study. *: data from a previous experimental investigation by the authors [38].

European Certification of ETICS, independent from the type of wall they are intended to be applied on. ETICS solutions are usually based on mineral or petrochemical materials such as hydrophobic mineral wool (MW) and expanded polystyrene (EPS).

4. Case studies and measurements on-site

4.1. Case studies

Three case studies were chosen for the investigation: the Municipal Library of Porto (in Porto, Portugal), the Coruchéus' library (in Lisbon, Portugal), and the Library of San Giorgio in Poggiale (in Bologna, Italy). The three buildings are characterized by massive masonry walls, traditionally constructed, and they are all conditioned with heating and cooling systems. They are located in areas with temperate climates with warm or hot summers and mild winters (temperature rarely or never going below 0 °C). The three case studies are shown in Fig. 2. As readable in their morphological configuration, they were originally constructed with the function of convent, residential palace and church, respectively. They were refurbished and readapted to new uses throughout the centuries, but no insulation was added to their walls in the interventions.

4.2. Measurements on-site

A variety of techniques for the characterization of hygrothermal performance of walls, as well as the diagnosis of existing problems, are nowadays available [41–46]. They are always recommendable before intervening on historic constructions and they provide for information that are valuable when designing the retrofit intervention.

In this work, the measurements performed on site were aimed to determine the boundary conditions to be used as input in numerical simulations, and to provide the data for their validation. Indoor air temperature and relative humidity were continuously recorded for one year, and the data were used to define annual boundary conditions at the interior side of the walls. The data obtained from local meteorological stations were used to define the yearly boundary conditions at the outdoor-facing side of the components.

Additional measures were performed for a period of 3–6 weeks, focusing on the air temperature in the close proximity of the walls, at both the interior and exterior side of the components. These data were used to compare the accuracy of results, when the air temperature in close proximity of the surface is used in boundary conditions, instead of the air temperature from meteorological stations and indoor monitoring. The interior and exterior superficial temperature of the walls was measured for the same period (3–6 weeks).

Superficial temperature of walls was the parameter considered in the
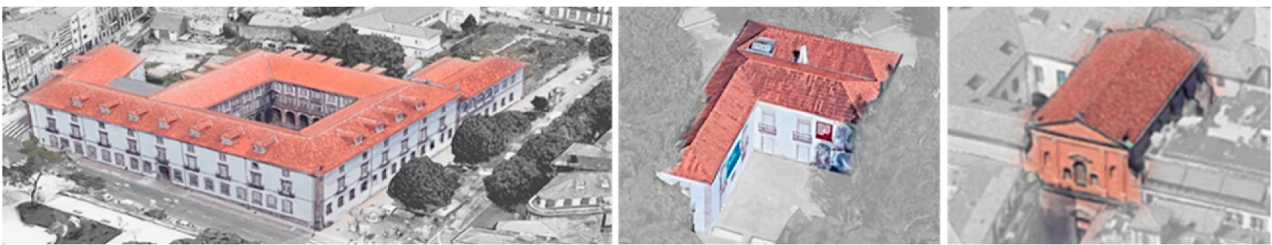

Fig. 2. – Aerial view of the Municipal Library of Porto, the Coruchéus Library and the Library of San Giorgio in Poggiale, adapted from Google Earth.
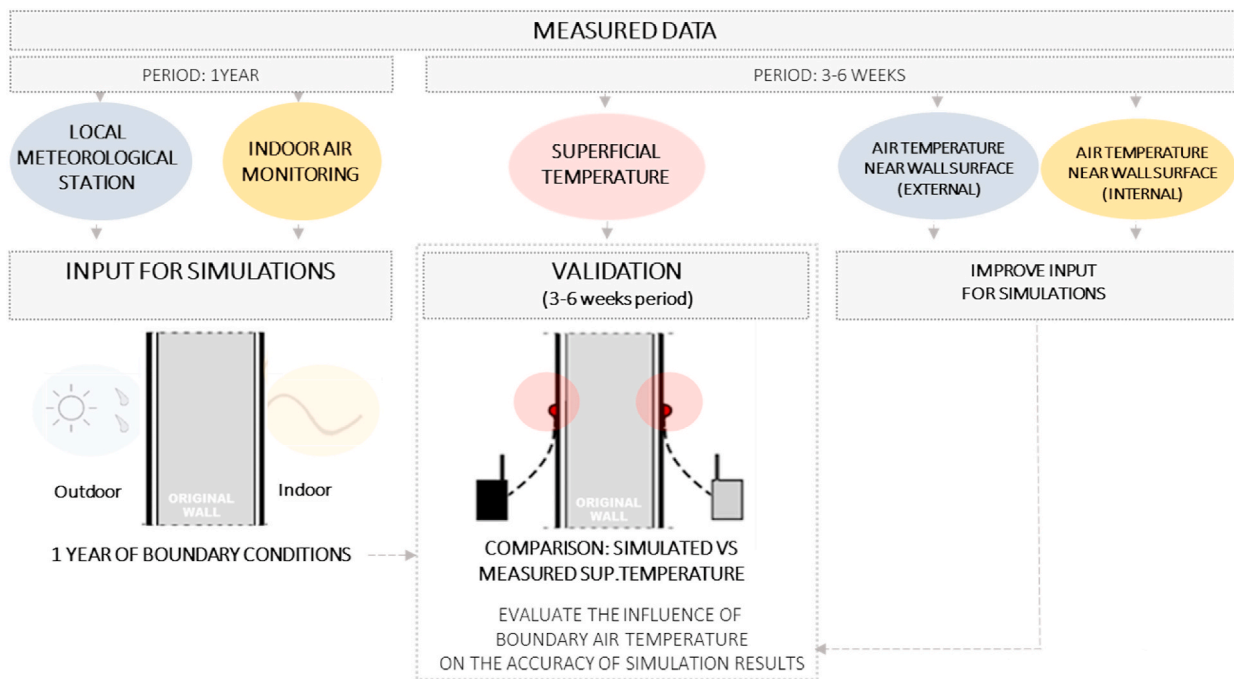

Fig. 3. – Method adopted to define the input and validate numerical simulations, based on data measured on-site.

validation of numerical simulations. The superficial temperatures measured on-site were compared to the results obtained in numerical simulations. The comparison allowed to discuss the accuracy of numerical simulations and validate them. The method adopted to define the input and validate numerical simulations, based on the data measured on-site, is showed in Fig. 3.

The methods adopted for the experimental monitoring are explained

in this section and the results are discussed in the following section, together with the simulation model, its input, and the validation process.

4.2.1. Indoor air temperature and relative humidity (1-year period)

Indoor air Temperature (T) and Relative Humidity (RH) were continuously recorded for one year in each case study, during regular usage of the buildings. In the two buildings located in Portugal, the
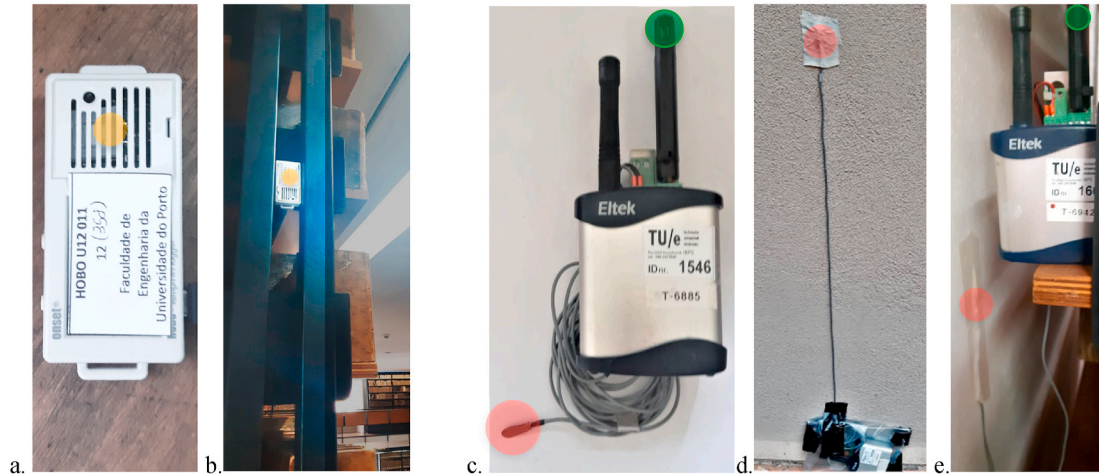

Fig. 4. Equipment adopted for the measurements on-site: (a) a HOBO datalogger U12-011 for air temperature and relative humidity, and (b) an example of installation in a bookshelf, (c) an ELTEK device with a sensor for air and superficial temperatures, and an example of the installation of the devices for measuring (d) the exterior and (e) interior superficial temperature of a wall. The sensors used for superficial temperature, air temperature, and for combined measures of air temperature and relative humidity are highlighted in red, green and yellow, respectively. (For interpretation of the references to colour in this figure legend, the reader is referred to the Web version of this article.)
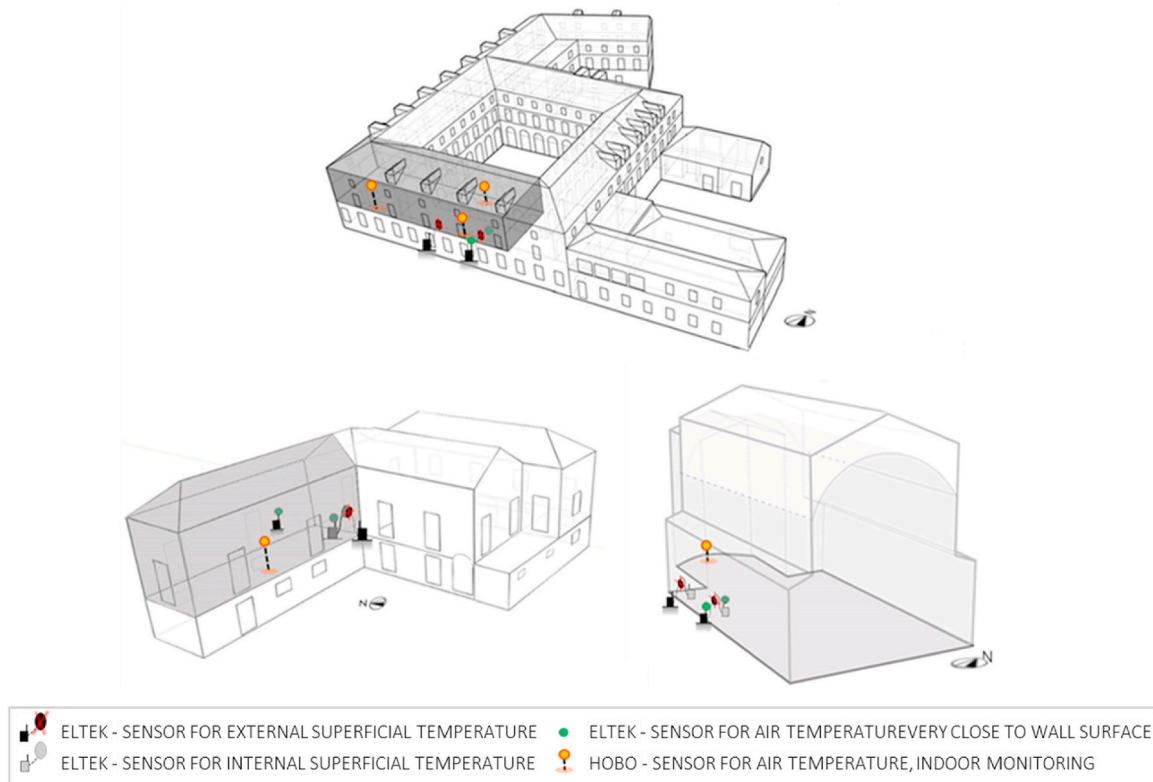
Fig. 5. From top to bottom, left to right: a grey pattern is adopted to indicate the room monitored in the Municipal Library of Porto, in the Coruchéus' Library and in the Library of San Giorgio in Poggiale. sensors In the first case study the devices used for the interior surface are not represented, for the reason of clarity of the image, but their position is symmetrical to the devices used outdoor. Red, green and yellow highlights are adopted to indicate the location of the sensors for superficial temperature (Eltek), air temperature (Eltek), and for air temperature and RH (HOBO), respectively. (For interpretation of the references to colour in this figure legend, the reader is referred to the Web version of this article.)

monitoring was performed from March 2019 to March 2020. In the Italian case study, the period January 2019 to January 2020 was considered. The monitoring was performed by means of dataloggers HOBO U12-013 (accuracy: ± 0.35 °C, and $\pm 2.5\%$ in the range 10–90% RH, 5% out of this range), which are shown in Fig. 4a and b. The sampling interval adopted was 10 minutes, and the results were defined as the hourly average of the measurements recorded. In the case study in Porto, 3 sensors were located nearby the building envelope, as shown in Fig. 5, and the indoor hygrothermal data of the room were obtained as the average of the three measurements. For the case study in Lisbon and Bologna, the data were obtained from a sensor located near an SW-oriented and a W-oriented wall, respectively. The equipment was positioned on top of bookshelves in the case studies of Porto and Lisbon, and behind an exposition box in the Library in Bologna. The positions were chosen to avoid the interference of users, drafts and solar radiation in the measurements.

4.2.2. Superficial temperature of the walls and air temperature near the interior and exterior surface of the envelope (3–6 weeks period)

In each case study, the internal and external superficial temperatures of one wall were monitored for at least three weeks. In the same period, the temperature of the indoor and outdoor air was recorded in points that were very close to the buildings envelope. The equipment adopted was Eltek sensors for air temperature (accuracy of ± 0.4 °C) and superficial temperature (accuracy of ± 0.3 °C). Measurements were collected through an Eltek RX250AL datalogger with a sampling interval of 10 min. Results were defined using the hourly averages obtained from the datasets. Fig. 4c shows one device equipped with the two sensors, while Fig. 4d and e displays an example of the installation on the interior and exterior side of the walls, respectively. The sensors for superficial temperature were applied on the surface of walls by means of adhesive tape. Between the sensor and the wall, a thermal paste (high thermal conductivity) was applied to guarantee continuous contact with the support.

External and internal air temperatures were measured very close to

the walls whose superficial temperature was monitored. The only exception is in the case study in Lisbon, where, for practical reasons, the sensor for external air temperature was located next to a North-oriented wall while the superficial temperature was measured for an SW-oriented one. In the case studies located in Porto and Bologna, the superficial temperatures were obtained as the average value of the measurements performed in two points on each surface, with two sensors, while in Lisbon only one sensor was used at each side of the wall, as schematically represented in Fig. 5.

5. Numerical model – description and validation

In this study, the Software WUFI Pro 5 [47] is adopted to perform mono-dimensional hygrothermal simulations of multi-layered walls cross-section under realistic climatic conditions. The software relies on Künzel's differential equations for the simultaneous transport of heat and moisture [48]. In WUFI Pro these equations are discretised by means of an implicit finite volume method and iteratively solved [49]. The model accounts for three types of moisture transfer: vapour diffusion, liquid transfer by absorption and liquid transfer by redistribution [50]. The software applies the dynamic outdoor weather and indoor climate as boundary conditions at the exterior and interior side of the building component, respectively. For each time step, the hygrothermal transfer across each material of the assembly is calculated [51], and the temperature and moisture content in each layer are consequently defined. WUFI Pro has been validated through several years of field and laboratory testing [52–56], and it is widely adopted to investigate the hygrothermal behaviour of historic and traditionally-constructed building components, as well as their retrofits [8,57–62]. The inputs required for the simulations are materials properties, geometry of the assembly and climatic boundary conditions (indoor and outdoor). Indoor climate conditions are simplified with hourly data of air temperature and relative humidity. The outdoor climate is defined through hourly data of air temperature, pressure and relative humidity, wind
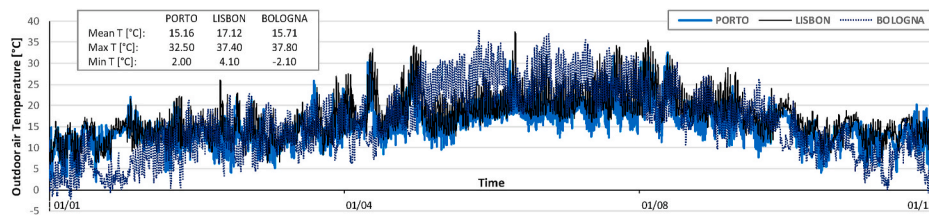

Fig. 6. Temperature in the Cities of Porto, Lisbon and Bologna, according to the data obtained from local meteorological stations.
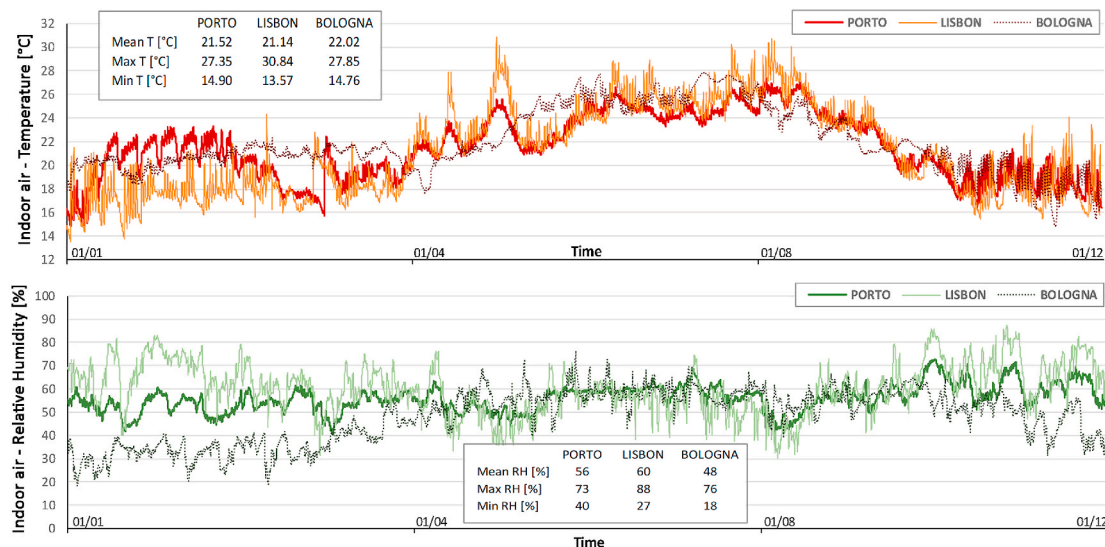

Fig. 7. Temperature and relative humidity: data set adopted for the indoor climate in numerical simulations, based on the indoor monitoring campaign.

speed and direction, solar radiation, and rain.

5.1. Description of numerical simulations

5.1.1. Boundary climatic conditions

The outdoor climate datasets were obtained as follows. For the cities of Porto and Lisbon, the weather data were provided by the *Portuguese Institute of Sea and Atmosphere* (IPMA), from weather stations located at about 11.5 km and 2.5 km from the case studies, respectively. For the city of Bologna, the hourly weather data were provided by the public entity ARPAE, which has a meteorological station at about 3 km from the third case study. Since the data concerning solar radiation were incomplete, the global and direct solar radiation data were taken from

the Test Reference Year (TRY) datasets. The TRY adopted for Porto is the one defined in Ref. [63]. For Lisbon and Bologna, the TRY was created with the software Meteonorm [64]. The datasets were constructed considering the same period used in the indoor monitoring campaign, namely March 2019–March 2020 for Porto and Lisbon, and January 2019–January 2020 for Bologna. The outdoor temperature in the three locations is reported in Fig. 6. It shows that Bologna has the coldest temperature in winter and the highest in summer. Porto and Lisbon have similar temperatures, with the former showing qualitatively colder conditions both in winter and summer.

At the interior side of the walls, the boundary conditions were defined according to the data measured on-site. This choice was taken to represent realistic operational conditions and to account for the
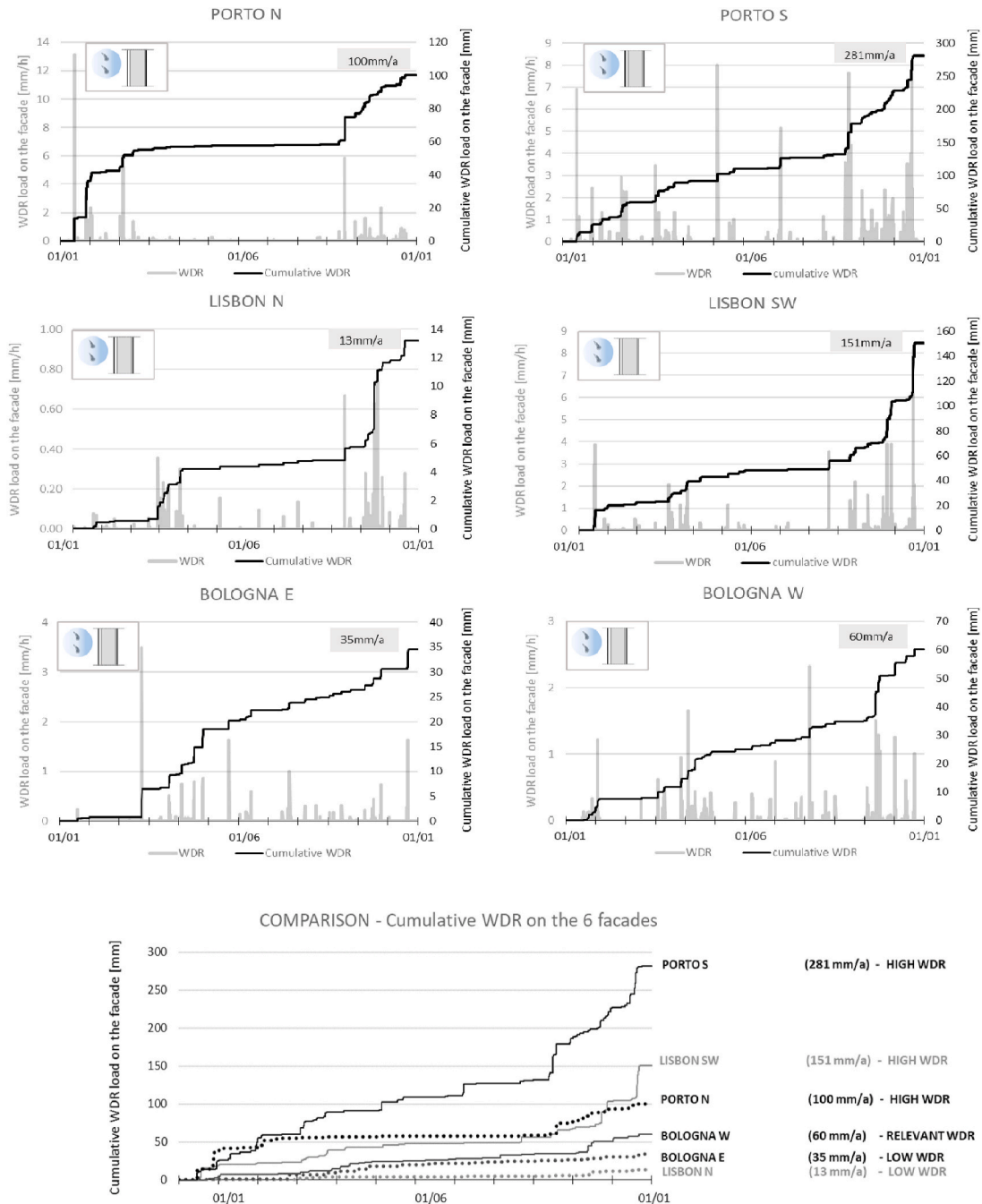

Fig. 8. Annual load of wind-driven rain in Porto, Lisbon and Bologna, for two specific walls orientations in each climate. The hourly load of WDR is shown in grey, and the cumulative load is displayed in black. The label on the top-right corner of each graphic indicates the annual sum of WDR on the façade. At the bottom: the cumulative WDR affecting the 6 facades.

fluctuations determined by occupancy and use of HVAC appliances. The dataset is presented in Fig. 7, and the main difference between the indoor climates seems to be the drier conditions that characterize the case study in Bologna during winter, which is likely to be the consequence of the higher use of heating.

5.1.2. Wind-driven rain

Given the importance of WDR (Wind-Driven Rain) for the moisture content of exposed walls [65], a detailed evaluation is provided for two wall orientations in each climate. The orientations were chosen to be representative of a higher and lower WDR load in each location. The WDR data were obtained starting from the measurements of local meteorological stations, according to the following calculation: $R_{WDR} = R_h \cdot (R_1 + R_2 \cdot V \cdot \cos(\psi))$, where R_{WDR} [mm/h] is the WDR intensity, R_h [mm/h] is the rainfall on horizontal surfaces, R_1[-] is the coefficient dependent on the surface inclination ($R_1 = 0$ for vertical components), R_2 [s/m] is the coefficient dependent on the vertical distance of the component from the ground (R2 = 0.07 up to 10 m of height [66]), V [m/s] is the average hourly wind speed at 10 m height, and ψ [°] is the angle between the wind direction and the normal to the façade. The WDR data are displayed in Fig. 8.

The graphics show that in Porto and Lisbon a relevant part of WDR is concentrated in the winter season, when a significant increase in the cumulative WDR is observable. On the contrary, WDR in Bologna is more evenly spread, having a noticeable increase of cumulative WDR also during summer. The annual load of WDR affecting the façades differs relevantly, with the South-oriented wall in Porto being affected by the highest annual WDR-load among the façades considered, namely about 281 mm/a (annual millimeters). For reasons of synthesis, in this work an annual sum of WDR above or around 100 mm/a is referred to as a high WDR load (walls in Porto and SW-wall in Lisbon). West-oriented walls in Bologna are considered as exposed to relevant WDR, which is about 60mm/a. North-oriented walls located in Lisbon and East-oriented ones in Bologna are referred to as affected by low or not-relevant WDR, which is below 40mm/a.

5.1.3. Walls assembly and simulation period

The tree walls considered in the study have different compositions, and thicknesses ranging from 60 to 90 cm. The wall located in Porto is the thickest one, and it is made of granite stone masonry. The wall in Lisbon is in rubble limestone masonry, whereases the wall in Bologna is in solid brickwork. Lime mortar joints are adopted in the three masonry walls. In addition, the interior and exterior surfaces of the walls are plastered and rendered, respectively.

The assembly of the walls and their main hygrothermal properties are provided in Table 1.

The materials' data are taken from the WUFI Pro database [67], except for the limestone, whose properties are based on an experimental study on Portuguese limestone [68]. Interior plasters and exterior renders are simplified using 3 cm of lime mortar, as assumed in Ref. [69] for Portuguese historic buildings. Since experimental investigations have shown that traditional mortars adopted in Portuguese historic construction for interior plastering and exterior rendering show similar characteristics and compositions [70–72], the same lime mortar is considered on both sides of the walls. According to the aforementioned studies, although the capillary absorption coefficient (A_w) of traditional lime mortars is quite variable, a good representation is given by an A_w in the range of 0.1–0.2 $kg/m^2s^{0.5}$ [24]. For this reason, a lime mortar with an A_w of about 0.17 $kg/m^2s^{0.5}$ was selected from the WUFI database. The materials adopted for the substrate of the walls located in Porto and Lisbon have thermal conductivities that are in good agreement with the indications given in the technical report "ITE 54 – Thermal transmission coefficients of building envelope elements" [73] for traditional Portuguese granite and limestone walls, i.e. a thermal conductivity of about 2.1 and 1.8 W/(m.K) respectively. In addition, the stone selected for the walls in Porto was chosen because of the similarity with the granite specimens observed in Ref. [74], which were extracted from historic walls. Similarly, the solid-brick masonry adopted for the wall of the case study in Bologna has a thermal conductivity that is consistent with the values observed in an extensive study on historic walls in Italy [75], i.e. 0.5–0.8 W/(m.K). An important difference between the three substrates lies in their capillary absorption coefficient, which indicates that the brick wall absorbs liquid water faster than limestone and granite components. Furthermore, the three materials have very different free saturation water contents, namely about 370 kg/m^3, 190 kg/m^3 and 40 kg/m^3, for bricks, limestone, and granite, respectively. Thus, bricks can store a much higher quantity of liquid water than the other two materials. These differences can be very important during rainy periods, especially for walls exposed to WDR and not protected with a water-resistant coating or a hydrophobic treatment, which is the scenario considered.

Although boundary conditions were defined for a 1-year-period, numerical simulations were run for a longer time, considering these boundary conditions to recur every year unchanged. Because of the repetition of the same yearly boundary conditions, after a certain period of time simulations reach dynamic equilibrium [6], meaning that the course of physical properties such as temperature and relative humidity in the walls does not change from one year to the next. After this steady annual performance is reached, simulation results do not depend on the initial conditions anymore, but only on the boundary climates [76]. For this reason, un-retrofitted walls were simulated for a 10-year-period of time, and the results presented in this work are those observed in the last year of simulations.

5.2. Validation of numerical simulations

5.2.1. Methods

The hygrothermal behaviour of the monitored walls was simulated, and the results obtained were compared to the superficial temperatures measured on-site. This comparison was used to provide a validation of

Table 1

Simulations of original walls configuration: assembly, materials, and boundary conditions.

External layer	Wall substrate	Internal layer	Indoor climate (measured on-site)	Outdoor climate (meteo-stations)
Lime plaster - 3 cm [67] (μ = 12, λ = 0.7 W/mK, A_w = 0.17 $kg/m^2s^{0.5}$)	Granite-90cm [67] (μ = 70, λ = 2.3 W/mK, [a]A_w = 0.002 $kg/m^2s^{0.5}$)	Lime plaster -3cm [67] (μ = 12, λ = 0.7 W/mK, A_w = 0.17 $kg/m^2s^{0.5}$)	Municipal Library of Porto	Porto
Lime plaster-3cm [67] (μ = 12, λ = 0.7 W/mK, A_w = 0.17 $kg/m^2s^{0.5}$)	Limestone-70cm [68] (μ = 41, λ = 1.3 W/mK, A_w = 0.02 $kg/m^2s^{0.5}$)	Lime plaster-3cm [67] (μ = 12, λ = 0.7 W/mK, A_w = 0.17 $kg/m^2s^{0.5}$)	Coruchéus Library	Lisbon
Lime plaster - 3 cm [67] (μ = 12, λ = 0.7 W/mK, A_w = 0.17 $kg/m^2s^{0.5}$)	Solid Brick-60cm [67] (μ = 15, λ = 0.6 W/mK, [a]A_w = 0.2 $kg/m^2s^{0.5}$)	Lime plaster -3cm [67] (μ = 12, λ = 0.7 W/mK, A_w = 0.17 $kg/m^2s^{0.5}$)	Library of San Giorgio in Poggiale	Bologna

Notation: μ - water vapour resistance factor, λ – thermal conductivity, A_w – capillary water absorption coefficient.

[a] Aw approximated from D_{ws} at free saturation (w_f) according to the formula $D_{ws}(w_f) = 3.8*(A_w/w_f)^2$ [48].

the simulation model adopted in this study. Validation is the process of assessing the physical accuracy of the model via comparing simulation and experimental results [77]. The validation process helps reducing the gap between simulated and real performance of building components [41–43] and makes the simulations more reliable for sensitivity and parametric studies [78].

First, the simulations were run considering the boundary conditions provided by the meteorological stations and the indoor monitoring campaign, as previously outlined. To assess the influence of temperature boundary conditions on the accuracy of results, the simulations were also performed by accounting for the indoor and outdoor air temperature measured very close to the walls with the ELTEK equipment, as shown in Fig. 3. The results obtained are provided in the following section. Simulated and measured superficial temperatures are compared via graphical representation, while the validation adopts statistical indexes.

Given the lack of consistent methodology or guidelines for the

validation of hygrothermal models in the context of historic constructions [79], the statistical quantification suggested in ASHRAE Guidelines 14: 2014 [80] is hereby considered. Although this method was originally defined for energy simulations, it is often adopted to evaluate the accuracy of hygrothermal simulations for historic buildings [4,81–85]. The statistical quantification is based on three indexes [82,86]:

- the Normalized Mean Bias Error - NMBE, which quantifies the global difference between the real values and the predicted ones (recommended to be within -10%, +10% - Hourly criteria);
- the Coefficient of Variation of the Root Mean Square Error - CV(RMSE), which indicates the model's ability to predict the overall load shape that is reflected in the data (suggested ≤30% - Hourly criteria);
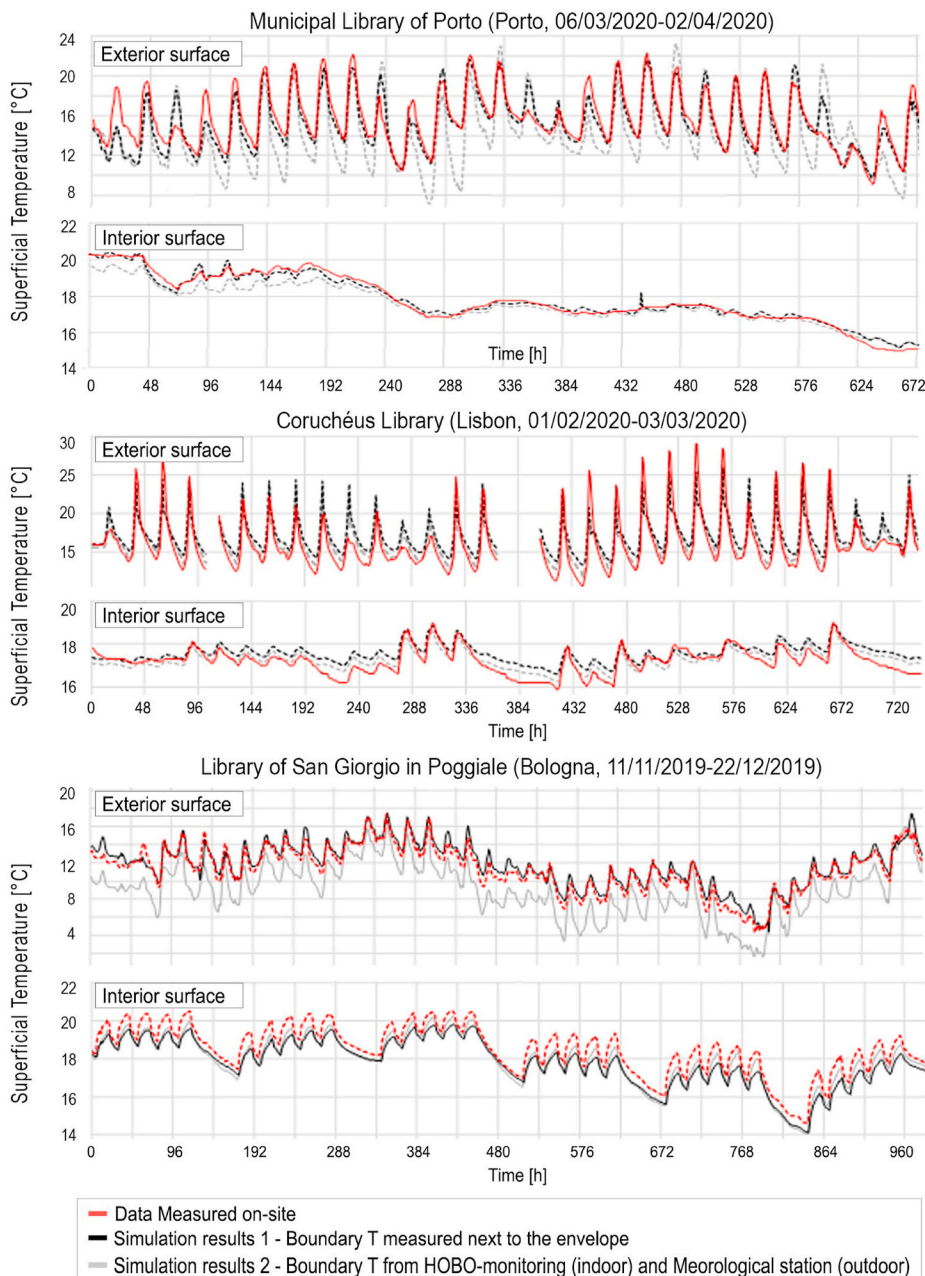

Fig. 9. External and Internal superficial temperature of walls: simulated and measured. The data missing in the graphic of the exterior surface temperature of the wall in Lisbon is the consequence of a data loss experienced due to technical problems.

Table 2

Simulated superficial temperature of the walls at their exterior (OUT) and interior (IN) surface - statistical quantification of the error. Simulations using the boundary conditions obtained from meteorological stations and the indoor monitoring or using the air temperatures recorded near the envelope are labelled as Sim1 and Sim2, respectively. Results that do not comply with threshold values are displayed in red.

VALIDATION: Comparison of the results of simulations performed with the original configuration of walls with the data measured on site for 3–6 weeks.				
	EXT.SURFACE		INT.SURFACE	
PORTO	OUT_Sim1	OUT_Sim2	IN_Sim1	IN_Sim2
	NMBE = 3% ≤ 10%	NMBE = 11%	NMBE = 0% ≤ 10%	NMBE = 2% ≤ 10%
	CV = 8% ≤ 30%	CV = 19% ≤ 30%	CV = 1% ≤ 30%	CV = 3% ≤ 30%
	$R^2 = 0.84 \geq 0.75$	$R^2 = 0.60$	$R^2 = 0.98 \geq 0.75$	$R^2 = 0.98 \geq 0.75$
LISBON	OUT_Sim1	OUT_Sim2	IN_Sim1	IN_Sim2
	NMBE = −6% ≤ 10%	NMBE = −2% ≤ 10%	NMBE = −2% ≤ 10%	NMBE = 0% ≤ 10%
	CV = 12% ≤ 30%	CV = 10% ≤ 30%	CV = 3% ≤ 30%	CV = 2% ≤ 30%
	$R^2 = 0.80 \geq 0.75$	$R^2 = 0.82 \geq 0.75$	$R^2 = 0.80 \geq 0.75$	$R^2 = 0.79 \geq 0.75$
BOLOGNA	OUT_Sim1	OUT_Sim2	IN_Sim1	IN_Sim2
	NMBE = −4% ≤ 10%	NMBE = 24%	NMBE = 4% ≤ 10%	NMBE = 3% ≤ 10%
	CV = 6% ≤ 30%	CV = 26% ≤ 30%	CV = 4% ≤ 30%	CV = 3% ≤ 30%
	$R^2 = 0.95 \geq 0.75$	$R^2 = 0.92 \geq 0.75$	$R^2 = 0.94 \geq 0.75$	$R^2 = 0.98 \geq 0.75$

- the coefficient of determination - R^2, which indicates how close simulated values are to the regression line of the measured values (recommended ≥0.75 for calibrated models).

For reasons of unavailability of the equipment, the superficial temperatures were measured for a relatively brief period, namely between 3 and 6 weeks. Thus, the validation accounts only for this period. Despite the brevity of the timespan considered, the validation is still considered as a useful tool for estimating the ability of the model to realistically predict the behaviour of the walls.

The validation has been done for the original walls. The original configurations of walls are provided in Table 1.

5.2.2. Results

A graphical comparison of the results obtained via measurements on site and through simulations is provided in Fig. 9. In the graphics, the superficial temperature measured on site is indicated in red. The data reported in grey are the results obtained in the simulations when the boundary conditions adopted are those recorded by local meteorological stations and the 1-year-long indoor monitoring (HOBO dataloggers). Results reported in black are those obtained when the boundary temperature conditions adopted are those measured next to the envelope with Eltek sensors (3–6 weeks). Due to technical problems, few days of data were not recorded on the external surface of the wall located in Lisbon, thus some data are missing in the corresponding graphic.

In all case studies, the superficial temperatures obtained via simulations have similar fluctuations and trends as the data measured on-site. In terms of temperature at the interior surface of the walls, results obtained with the different boundary conditions (data represented in grey and black) are quite similar. This outcome suggests that the temperature observed in the indoor monitoring campaign (HOBO equipment) is similar to that measured very close to the walls (ELTEK equipment). Results obtained at the exterior surface of walls show more relevant differences. Results in grey (simulations with climate data from meteorological stations) are tendentially lower than those in black (simulations with ELTEK data for outdoor air temperature). This outcome is likely to be the consequence of the position of the meteorological stations. They are indeed located outside the city centres, where the microclimate can be slightly different from the one in the neighbourhoods of the case studies. For the libraries located in Porto and Bologna, the exterior temperature is more accurately predicted when the boundary outdoor conditions consider the temperature measured near the envelope, rather than the one detected by local meteorological stations. For the case study in Lisbon, results obtained with the two different external boundary conditions are both very close to the data measured on-site.

The statistical quantification of the errors is reported in Table 2. All simulation results, independently from the boundary conditions adopted, comply with the indication of ASHRAE guidelines for statistical errors – in terms of temperature at the interior surface of walls. For
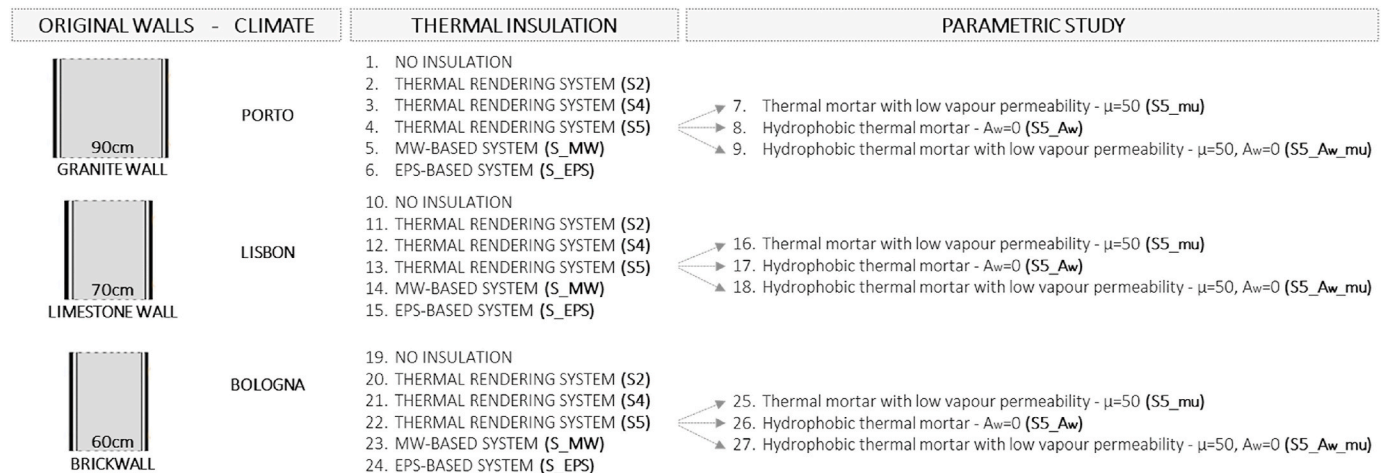
ORIGINAL WALLS - CLIMATE	THERMAL INSULATION	PARAMETRIC STUDY
90cm GRANITE WALL — PORTO	1. NO INSULATION 2. THERMAL RENDERING SYSTEM (S2) 3. THERMAL RENDERING SYSTEM (S4) 4. THERMAL RENDERING SYSTEM (S5) 5. MW-BASED SYSTEM (S_MW) 6. EPS-BASED SYSTEM (S_EPS)	7. Thermal mortar with low vapour permeability - μ=50 (S5_mu) 8. Hydrophobic thermal mortar - Aw=0 (S5_Aw) 9. Hydrophobic thermal mortar with low vapour permeability - μ=50, Aw=0 (S5_Aw_mu)
70cm LIMESTONE WALL — LISBON	10. NO INSULATION 11. THERMAL RENDERING SYSTEM (S2) 12. THERMAL RENDERING SYSTEM (S4) 13. THERMAL RENDERING SYSTEM (S5) 14. MW-BASED SYSTEM (S_MW) 15. EPS-BASED SYSTEM (S_EPS)	16. Thermal mortar with low vapour permeability - μ=50 (S5_mu) 17. Hydrophobic thermal mortar - Aw=0 (S5_Aw) 18. Hydrophobic thermal mortar with low vapour permeability - μ=50, Aw=0 (S5_Aw_mu)
60cm BRICK WALL — BOLOGNA	19. NO INSULATION 20. THERMAL RENDERING SYSTEM (S2) 21. THERMAL RENDERING SYSTEM (S4) 22. THERMAL RENDERING SYSTEM (S5) 23. MW-BASED SYSTEM (S_MW) 24. EPS-BASED SYSTEM (S_EPS)	25. Thermal mortar with low vapour permeability - μ=50 (S5_mu) 26. Hydrophobic thermal mortar - Aw=0 (S5_Aw) 27. Hydrophobic thermal mortar with low vapour permeability - μ=50, Aw=0 (S5_Aw_mu)

Fig. 10. Configurations considered in the comparative study.

external superficial temperatures, the statistical indexes confirm that simulations results fit very well with the measurements performed on-site, when outdoor boundary temperature is based on the measurements taken near the building envelope (results presented in black in Fig. 9). Results obtained using the weather data from the meteorological stations have a worse fit. For the case study located in Lisbon, the indexes of error comply with ASHRAE indication when both types of outdoor boundary thermal conditions are considered. For the other two case studies, the simulations are evaluated as validated and suitable for the scope of the study, even though some results do not comply with the ASHRAE indications. This assumption is taken for the following reasons. The CV complies with the threshold value, showing that the overall load-shape of the data is well predicted. The NMBE is positive, meaning that the simulations underestimate the external superficial temperatures, thus safely increasing the predicted risks related to moisture accumulation and reduced drying capacity.

Maximum absolute errors are in the range of $\pm 1.3\,°C$ and $\pm 7.7\,°C$, at the interior and exterior surface respectively. The 95th percentile of the distribution of absolute errors falls below $4.6\,°C$ for exterior superficial temperatures, and $0.9\,°C$ for temperatures at the interior surface of walls.

6. Comparative assessment - materials and methods

In the comparative study, simulations are run considering the original walls (no insulation) and the walls insulated with five different external insulation solutions. A parametric study is also performed, altering the hygric properties of one thermal mortar. Results are discussed in terms of moisture-related risks.

The configurations considered in the comparative study are reported in Fig. 10, and they are 27 in total.

In the following paragraphs, the materials adopted in the thermal insulation solutions are introduced. Then, the properties of the complete insulation systems are compared to those recommended in two

regulations for rain protective stuccos and ETICS.

6.1. Materials and systems

The thermal mortar-based systems considered are the ones characterized in a previous experimental campaign [38] on thermal insulation solutions suitable for application on historic walls, and they are presented in detail in Table 3.

Following the nomenclature adopted in the study, the systems hereby considered are the following. Two systems relying on cork-based renders, S2: A1 + B1 + C2 and S4: A2 + B1 + C2, where A1 and A2 are lime-cork mortars, B1 is a regularization mortar, and C2 is a potassium silicate paint reported to be vapour permeable and water-resistant by the manufacturer. The last system (S5: A3 + B2) is made of a thermal mortar with EPS aggregates and mixed binders (A3), covered with a regularization mortar that also works as finishing layer (B2). These systems are compared to others based on more common insulation materials: Hydrophobic mineral wool (MW) and Expanded Polystyrene (EPS). MW and EPS are non-hygroscopic materials with very low capillary absorption coefficients (A_w). They respectively have high and low water vapour permeability. The two materials have such low A_w, less than $0.008\ kg/m^2s^{0.5}$ according to the tests performed in Ref. [87], that their suction and redistribution coefficients, which govern liquid transport in the materials, are simplified as null in the WUFI database for insulation materials. In order to simplify the comparison, the theoretical systems S_EPS and S_MW are composed of a layer of insulation (respectively EPS and MW) and a coating layer made of B2, similar to system S5. A visual representation of the systems is provided in Fig. 11.

In order to evaluate how capillary absorption coefficient and water vapour permeability affect moisture-related risks, one of the thermal mortars (A3) is used for a parametric study, by altering its hygric transport properties. Thus, three auxiliary systems are considered: S5_mu, where thermal mortar A3 is given a $\mu = 50$, i.e., the same high

Table 3
Thermal insulation solutions: systems assembly and hygrothermal properties of single materials.

Systems	Assembly (nomenclature: m. = mortar, reg. = regularization, fin. = finishing)						
S2	Thermal m. A1(4 cm) + reg. m. B1 (2 mm) + paint C2 (0.5 mm)						
S4	Thermal m. A2(4 cm) + reg. m. B1 (2 mm) + paint C2 (0.5 mm)						
S5	Thermal m. A3(4 cm) + reg./fin. m. B2 (2 mm)						
S_MW	Mineral wool MW(4 cm) + reg./fin. m. B2 (2 mm)						
S_EPS	EPS(4 cm) + reg./fin. m. B2 (2 mm)						
S5_mu	Thermal m. A3 with $\mu = 50$ (4 cm) + reg./fin. m. B2 (2 mm)						
S5_A_w	Thermal m. A3 with Aw = 0 and null sorption isotherm (4 cm) + reg./fin. m. B2 (2 mm)						
S5_A_w_mu	Thermal m. A3 with $\mu = 50$, Aw = 0 and null sorption isotherm (4 cm) + reg./fin. m. B2 (2 mm)						

Material property	Single materials							
	A1	A2	A3	B1	B2	C2	MW	EPS
Dry bulk density [kg/m³]	612.8	724.2	342.3	1617	1316	1617	60	30
Open porosity [−]	0.342	0.307	0.288	0.307	0.311	0.307	0.950	0.950
Water vapour resistance coefficient [−]								
- Dry cup	14.6	18.8	11.0	18.3	15.6	737	1.3	50
- Wet cup	12.0	14.7	9.17	13.4	13.7	648	/	/
Capillary water absorption coefficient [kg/(m² s⁰·⁵)]	0.044	0.022	0.034	0.18	0.034	0.0046	0	0
Free water saturation [kg/m³]	300.0	215.9	66.2	276.7	128.6	276.7	0	0
Moisture storage function [kg/m³]	[38]	[38]	[38]	[38]	[38]	[38]	0	0
Water content (w) at 80%RH [kg/m³]	18.42	17.91	14.30	12.18	16.02	6.69	0	0
Specific heat capacity [J/(kg.K)]	843	848	920	850	850	850	850	1500
Thermal conductivity dry [W/(m.K)]	0.0978	0.128	0.0654	0.7	0.7	0.7	0.04	0.04
Thermal conductivity moisture-dependent (Water content [kg/m³]; Th. Conductivity [W/(m.K)])	[38]	[38]	[38]	/	/	/	(300.0; 0.01), (600.0; 0.27), (900.0; 0.55)	(300.0; 0.01), (600.0; 0.24), (900.0; 0.52)

Main properties of the underlined original lime render considered in the simulations:
Dry bulk density = 1600.0 kg/m³, Open porosity 0.330, Vapour resistance factor (dry cup) = 12.0,
Moisture storage function (RH,water; content in kg/m³) = (0%; 0.0), (50%; 9.3), (65%; 16.0), (80%; 24), (99%; 85), (99.5%; 89), (99.9%,98), Water content (w) at 80%RH = 24 kg/m³, Specific heat capacity 850.0 J/(kg.K), Thermal conductivity dry 0.7 W/(m.K), Thermal conductivity moisture-dependent – linear correlation from (0 kg/m³; 0.7 W/m.K) to (330 kg/m³;1.234W/m.K).

THERMAL RENDERING SYSTEMS

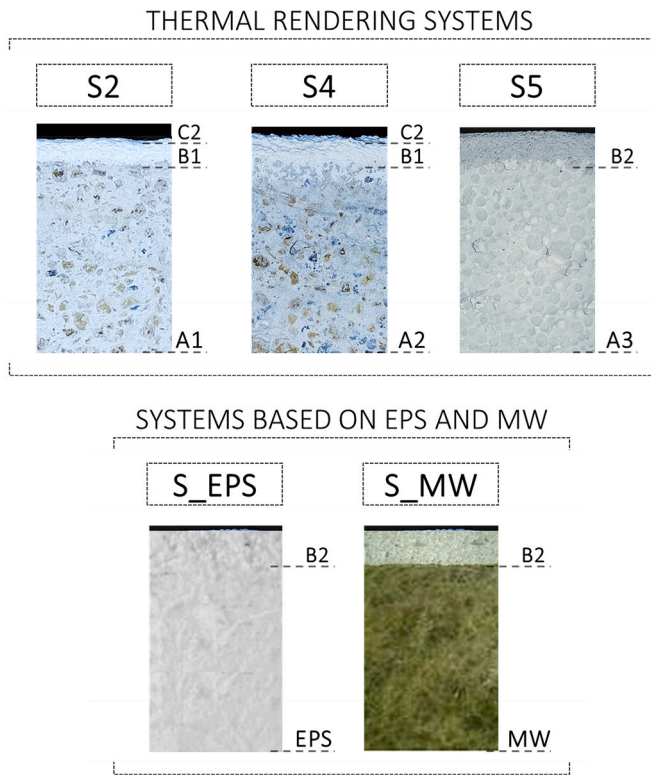## SYSTEMS BASED ON EPS AND MW

Fig. 11. Picture of thermal rendering systems S2, S4 and S5, and a representation of theoretical systems S_EPS and S_MW, adapted from similar components used in Ref. [88]. Legend: A1, A2, A3 - thermal mortars, B1, B2 - regularization mortars, C2: paint, EPS: expanded polystyrene, MW: hydrophobic mineral wool.

water vapour resistance factor of EPS; S5_A_w, where A3 has $A_w = 0$ and a null sorption isotherm (non-hygroscopic), i.e. the same as EPS and hydrophobic mineral wool; S5_A_w_mu, where thermal mortar A5 is assigned with a $\mu = 50$, $A_w = 0$ and a null sorption isotherm, like EPS. The s_d and A_w of these three systems are schematically reported in Fig. 12.

For practical reasons, in this work materials with moderate (not null) or high A_w and not null sorption isotherm are referred to as capillary active and hygroscopic, as opposed to hydrophobic and non-hygroscopic materials such as EPS and MW. All insulation systems have a 4cm-thick
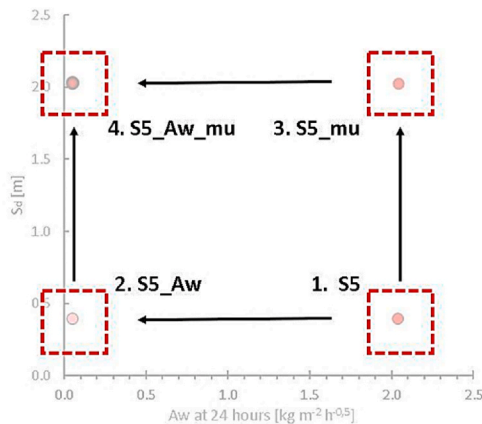

Fig. 12. Systems adopted in the parametric study i.e., those obtained from the modification of the hygric properties (equivalent air layer thickness, s_d, and capillary absorption coefficient, A_w) of system S5.

insulation layer. The assembly considered for each insulation system and the hygrothermal properties of single materials are provided in Table 3. All insulation systems are in direct contact with the wall substrate. Thus, the intervention simulated is the removal of the original render, and successive application of the external thermal insulation system. For thermal mortars, it is common practice to apply the material on the wall, directly. For EPS and MW, various types of installation can be considered, for instance the use of an adhesive layer or mechanical fastening systems. In this study the latter is considered, to make the comparison with thermal mortars more direct, since no additional layer of glue is introduced. Finally, the simulations are run under the hypothesis of perfect contact between the insulation layer and the surface of the wall.

In Table 3, the main hygrothermal properties of the original render are also provided.

6.2. Hygric properties of complete insulation systems

The capillary absorption coefficient and resistance to water vapour diffusion of exterior insulation systems have mayor impact on the moisture dynamics of exposed walls, since they regulate the wetting and drying of components. The importance of these two parameters for outdoor-exposed building elements emerges in two regulations. The European Assessment Document for External Thermal Insulation Composite Systems (ETICS) with renderings - EAD 040083-00–0404:2020 [40], and the German standard DIN 4108–3:2018 on rain-protective stuccos and coatings [39,89]. The first regulation sets a maximum capillary absorption for complete insulation systems (A_w of 0.10 kg m^{-2} h$^{-0.5}$), and a maximum s_d (water vapour diffusion equivalent air layer thickness) of 1 m for the coating render of vapour permeable insulation materials. The second standard defines a hyperbola A_w*s_d = 0.2 kg m^{-1} h$^{-0.5}$, and all solutions having a lower A_w*s_d are considered suitable to avoid moisture accumulation in masonry walls, because of their good balance between rainwater intake and drying. In the same standard, a maximum value is also set for the A_w and s_d of stuccos and coatings, namely 0.5 kg m^{-2} h$^{-0.5}$ and 2 m. The A_w and s_d of the original render and of the external insulation systems considered in the simulations are displayed in Fig. 13, together with the recommendations mentioned for ETICS and rain-protective stucco/coatings.

From Fig. 13 it emerges that three systems comply with the limits set in the German standard: S5, S_MW and S5_A_w_mu. The latter two systems are also below the threshold values of the EAD for ETICS, because of their very low capillary absorption coefficient and high water vapour permeability. Three systems fall out of the German-hyperbola, namely S2, S4 and S5_mu. Two systems exceed the recommendations of the German standard because of their high s_d value (S5_A_w_mu and S_EPS), despite being below the hyperbola A_w*s_d = 0.2 kg m^{-1} h$^{-0.5}$. The original plaster greatly exceeds the maximum capillary absorption coefficient considered in the German standard, while having a very reduced s_d, meaning that it does not provide for relevant protection against rainwater intake, but it allows for the wall substrate to dry quite fast, thanks to its low resistance to water vapour diffusion.

6.3. Simulation period and initial hygrothermal conditions in the walls

The retrofitted scenarios are simulated considering the application of insulation on the original moist wall. Two scenarios are evaluated, considering different initial moisture contents in the walls substrate. First, simulations are run considering a realistic initial moisture content, which is approximated by using a significatively high water content observed in the un-retrofitted walls at dynamic equilibrium conditions. The results of these simulations are adopted to evaluate moisture accumulation risk. The second type of simulation accounts for a very high initial moisture content, which is approximated with saturation conditions in the wall substrate. Results obtained in this scenario are used to discuss the risk of reduced drying entailed by the insulation. All
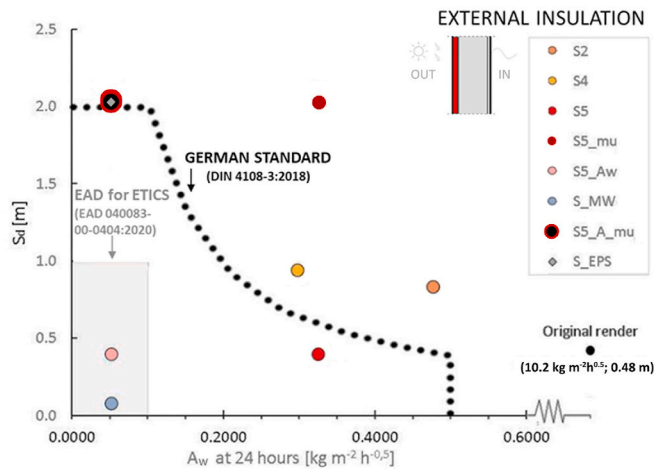
Fig. 13. Equivalent air layer thickness (s$_d$) and capillary absorption coefficient (A$_w$) of external insulation systems and original render. The black dotted line represents the recommendation of the German standard DIN 4108-3 and the grey area indicates the values below the maximum threshold references mentioned in the EAD for ETICS.

simulations of retrofitted walls start from the 1st of January and they are run for a 10-year-long period.

6.4. Assessment criteria

It is very well known that the best way of insulating a wall is to apply the insulation to the exterior surface [6]. Indeed, this intervention can help to decrease the intake of wind-driven rain while keeping the wall warmer during the heating season. On the other hand, external insulation can significantly reduce the drying of the component through its external surface because of the increased resistance to water vapour diffusion. In order to assess whether the retrofit interventions entail moisture-related risks, the results of the simulations are analyzed in terms of moisture accumulation in the wall substrate and reduction of drying. Results are presented and discussed in terms of saturation degree in the wall substrate, calculated as the ratio between the water content and the free saturation water content of the material [%], thus representing the fraction of open pores filled with moisture against those accessible for moisture [90]. This parameter is adopted to make results comparable, since the walls considered have substrates characterized by very different saturation water contents and open porosities. The term water/moisture content is adopted to indicate the mass of water contained in the unit of volume of material.

6.4.1. Moisture accumulation

Since post-insulating an existing wall entails a change in its heat and moisture transfer, it can lead to an increase in moisture content. This risk is qualitatively evaluated by comparing the water content in the wall substrate (granite, limestone, bricks) in the original configuration, at dynamic equilibrium, and during a 10-year-period for retrofitted configurations. An index for evaluating the risk (i$_{m.a.}$) is hereby defined as:

$$i_{m.a.} = \frac{w_{avg_{retrofitted}} - w_{avg_{un-retrofitted}}}{w_{avg_{un-retrofitted}}} \ [\%] \tag{1}$$

where w$_{avg\_un-retrofitted}$ and w$_{avg\_retrofitted}$ indicate, respectively, the average annual water content in the substrate of the un-retrofitted wall at dynamic equilibrium, and in the retrofitted wall during the 2nd year of simulations. The greater the index the higher the increase of water content in the wall, while negative results indicate that the retrofit leads to a reduction of average annual water content in the wall.

6.4.2. Reduction of drying

When adopting thermal insulation systems for retrofitting exposed walls, the risk of having a reduction of drying should be considered [6]. Safeguarding the original drying ability of traditionally constructed walls is always important, even for walls protected from wind-driven rain, since all walls may suffer from dampness due to other causes such as rising damp, damages in the envelope, pipes leakage or even floods, a concern that is growing with the worsening of climate change [91]. What is more, interventions that reduce the drying ability of walls can determine an increased level of rising damp [92]. The drying of walls is hereby studied considering walls starting from saturation water content and drying under operational conditions. The drying abilities of the original and retrofitted walls are qualitatively compared by plotting the water content in the wall substrate during 10 years of drying from saturation. A numerical index is adopted to compare the reduction of drying entailed by the different retrofit solutions. The index (i$_{drying}$) is hereby defined as:

$$i_{drying} = \frac{w_{d\_avg_{retrofitted}} - w_{d\_avg_{un-retrofitted}}}{w_{d\_avg_{un-retrofitted}}} \ [\%] \tag{2}$$

where w$_{d\_avg\_un-retrofitted}$ and w$_{d\_avg\_retrofitted}$ indicate the average water content in the substrate of the un-retrofitted and retrofitted wall, respectively, during the 2nd year of drying. The higher the index the stronger the reduction of drying, whereas a negative index indicates that the retrofitted wall dries faster than in the original configuration.

The indexes adopted refer to the second year of simulations. This choice is taken to represent the wall condition after one year from the retrofit intervention.

6.4.3. Matrix of moisture-related risks

The results obtained in the study are synthesized by means of a matrix of indexes. A colour scale is used to improve the readability of the results. The range found between the maximum and minimum risk index in the matrix is divided in sub-ranges, corresponding to a colour from red to green accordingly to the level of risk, from high to low, similar to the assessment colour scale suggested in standard EN 16883:2017 – Guidelines for improving the energy performance of historic buildings [63].

6.5. Limitations of the study

This study accounts for the plane behaviour of perfect walls and it does not refer to room corners, cracks in walls, window recesses, and other thermal bridges areas where the temperature can get very low during the cold season. The behaviour of masonry walls is simplified through the use of a uniform material, thus neglecting the presence of interlayer connections (mortar joints through bricks or stones), as commonly assumed in numerical simulations [6,89,93,94]. These limitations are relevant but acceptable, since this study aims at providing a comparative evaluation of different insulation solutions. Similar rankings from the best to the worst behaviour of the systems are expected when real applications, including thermal bridges and joints, are considered. Future studies should be devoted to furtherly investigate the suitability of thermal renders for application on traditional and historic walls by means of experimental applications on existing buildings.

7. Comparative assessment – results and discussion

7.1. Moisture accumulation

In Fig. 14 the saturation degree in the walls located in Porto, Lisbon and Bologna is presented, from top to bottom. On the left and right sides of the figure, the results obtained with walls exposed to higher and lower annual loads of WDR are reported, respectively.

In the un-retrofitted walls (continuous black line), the lowest saturation degrees (always below 5%) are found in the N-oriented wall in

Lisbon and in the two walls located in Bologna. In Lisbon, the moderate water content is the result of the low annual load of WDR. In Bologna it seems the result of the moderate annual load of WDR and the fact that it is spread along the year, being relevant during summer, when water can better evaporate because of the higher temperatures. Much higher moisture content is found in the walls of Porto and in the SW-oriented façade in Lisbon, where the load of WDR is significantly high. Water content is especially high in the S-oriented wall in Porto, where the WDR load is about two to three times higher than in the other façades exposed to high WDR. Saturation degrees are roughly in the range 35–45% in the former wall and 20–30% in the latter ones. These values appear relevant. They are more than one order of magnitude higher than practical moisture content (i.e., content at 80% RH, which is about 2% and 0.7% for the substrate of Porto and Lisbon walls, respectively). In addition, a saturation degree of 30% corresponds to an increase of about 20% in thermal conductivity in these walls, in comparison to dry conditions. This result suggests that reducing the water content can be very beneficial for the thermal performance of these three walls.

In the retrofitted walls, it seems that adopting external thermal insulation in façades exposed to low WDR results in neglectable changes of saturation degree. On the contrary, for façades exposed to relevant or high WDR, the effect of the external insulation on the moisture content of the wall is very significant. The adoption of S_EPS and S_MW reduces moisture content to a higher extent than any other insulation solution, in all walls. This seems the result of the very low A_w of these two systems, which decreases rainwater intake in the façades. The highest benefits are observed in walls exposed to high WDR, where the saturation degree falls to about ½ of the initial value in the walls located in Porto, and less than 1/5 in the SW-oriented façade in Lisbon, at the end of the 10-year-period. In the three walls exposed to high WDR, S_MW leads to a lower saturation degree than S_EPS. This result is likely to be related to the much lower s_d that S_MW has, which positively affects the drying ability of the wall through vapour diffusion.

Also with thermal mortar-based systems the outcomes depend on the WDR affecting the walls. The three systems S2, S4 and S5 do not result in relevant changes of saturation degree in walls exposed to low WDR. In the W-oriented wall in Bologna, which is subjected to relevant WDR, the reduction of rainwater intake provided by S5 is evident and the peak of saturation degree is reduced, but the minimum water content stays at the same level as in the un-retrofitted wall. This outcome shows that although reducing rainwater intake, S5 slightly slows down the drying of the wall. The effect of S2 and S4 on reducing the peak of saturation degree in the wall is very similar to S5, but they entail a much stronger reduction in the drying ability of the component. For this reason, they lead to noticeably higher water content than in the original wall, for most of the time. In walls exposed to high WDR, system S5 leads to a strong reduction of water content through the 10-year-period considered, which is the result of the protection from rain provided and the moderate impact on drying. On the contrary, systems S2 and S4, slow down the drying to a very relevant extent, thus leading to higher water contents than S5, and even higher than in the un-retrofitted walls for Lisbon SW and Porto N façades. In these two walls, water accumulation is observed when systems S2 and S4 are adopted, with the saturation degree of the wall getting higher year by year. In the S-oriented wall in Porto, the systems do not lead to higher water contents than in the original wall. In this case, the balance between the reduced rainwater intake and the slower drying is more favourable than with the original render. This outcome seems the result of the very high WDR affecting the façade, which probably makes the reduction of rainwater intake provided by S2 and S4 more relevant than the reduction of drying entailed.

The results obtained in the parametric study on hygric properties of S5 are reported in Fig. 15.

In the picture, black lines represent the saturation degree in the walls substrate when the un-retrofitted configuration is considered. In all cases, the best results are obtained when system S5 has a low water absorption coefficient ($S5\_A_w$ and $S5\_A_w\_mu$). Furthermore, lower water contents are observed with $S5\_A_w$ than $S5\_A_w\_mu$, in the S-oriented wall in Porto and in the SW-oriented façade in Lisbon. This result suggests that even with a reduced intake of rainwater, the walls have a slower drying when the s_d of the system is high, which is consistent with the
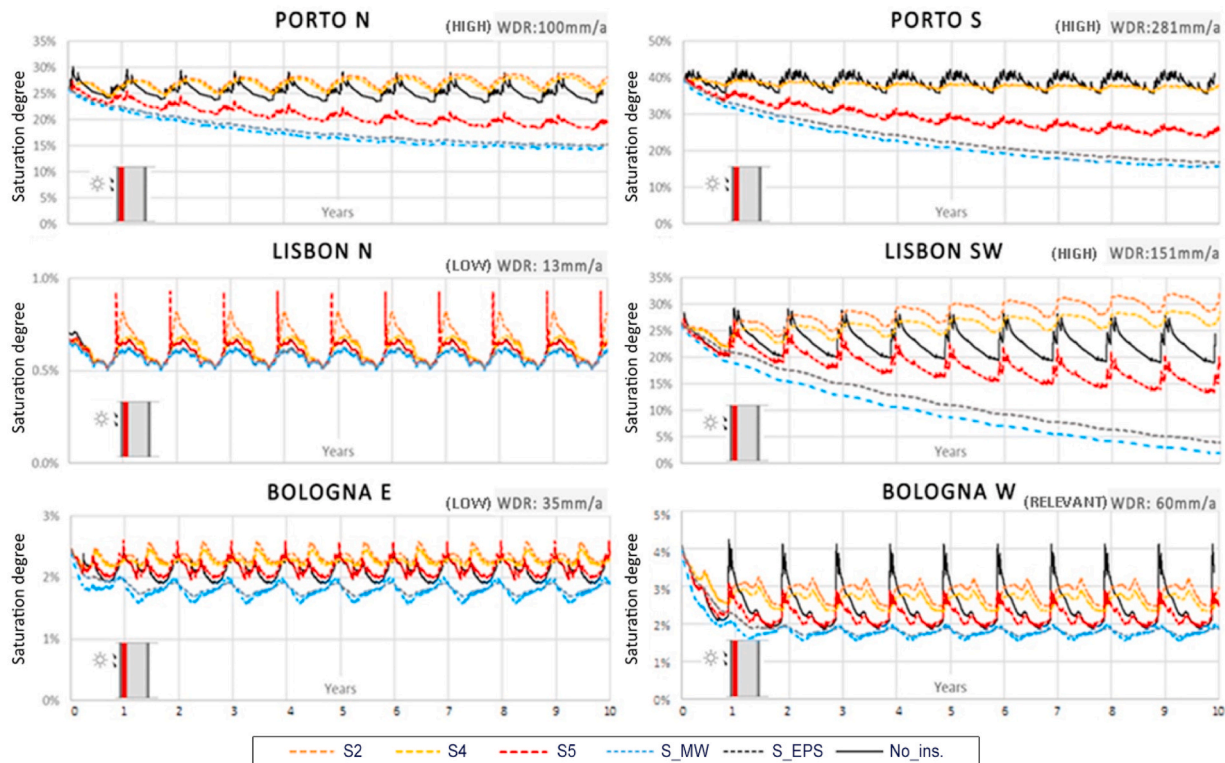

Fig. 14. Saturation degree in walls substrate in the original and retrofitted scenarios (external insulation).

outcomes previously obtained in the comparison between S_EPS and S_MW. S5_mu determines higher water contents than S5, but to an extent that does not appear relevant, in most walls. The moderate impact of S5_mu on moisture content, despite its high s_d, is probably due to the reduction of rainwater intake, which appears more relevant than the reduction of drying entailed, under typical operational conditions. Overall, the impact of a low A_w seems more significant than the impact of a high s_d in walls exposed to high wind-driven rain. Nonetheless, in the walls of Bologna, S5_mu determines noticeably higher moisture content than S5 and the original render, but the saturation degree remains so low that the increase does not seem relevant.

In conclusion, the results obtained with external thermal insulation systems and in the parametric study suggest that the impact of the systems on moisture content in the walls depends on their effect on rainwater intake and drying of the component. The outcomes are consistent with the recommendations provided in the German standard for rain-protective stuccos and coatings, and in the EAD for ETICS. Indeed, the only systems that determine a noticeable increase in the moisture content in some of the walls are the three systems that do not comply with the hyperbola defined in the German standard: S2, S4, and S5_mu (only in the Bologna E wall), with the former two even leading to moisture accumulations in two walls. The best results are obtained with systems that comply with the stricter limits defined in the EAD for ETICS, namely S_MW and S5_A_w, thanks to their very reduced s_d and A_w. S_EPS and S5_A_w_mu are the only systems that exceed the maximum s_d allowed in the German standard, while complying with the recommended hyperbola. The high resistance to vapour diffusion of the systems does not appear problematic when operational conditions and typical moisture contents are considered. Nonetheless, it might be concerning during drying from high water content. This behaviour is evaluated in detail in the next section.

Finally, it is worth underlying the importance of the finishing adopted in thermal rendering solutions. Systems S2 and S4, which show the worst performance, are finished with a silicate paint that was supposed to be vapour permeable considering the manufacturer information, but proved in fact to have a relevant resistance to water vapour diffusion (C2) in experiential tests [38]. On the contrary, system S5 is coated with a finishing mortar characterized by a high water vapour permeability (B2). The different finishing is very likely to be responsible for the different hygric behaviour of the systems. To investigate this point, some complementary simulations were run considering different finishings for the rendering systems, on the walls of Lisbon. Results are reported in ANNEX I and they show that all the three thermal mortars considered (A1, A2, A3) provide for good performance when finished with the coating B2, while they do not when finished with paint C2. Also in this case results are consistent with the recommendations of the German standard, since all systems finished with B2 comply with the hyperbola $A_w * s_d = 0.2$ kg m^{-1} h$^{-0.5}$, while systems finished with the second coating (B1+C2) do not.

7.2. Reduction of drying

The saturation degree observed during the drying from saturation, in the retrofitted and un-retrofitted scenarios, are displayed in Fig. 16. The black lines indicate the results obtained without insulation; all the others represent the scenarios retrofitted with different external thermal insulation systems.

S_EPS determines higher water content than in the un-retrofitted walls, and higher than all other insulation systems, for at least the first two years after the application. This result indicates that a system with a high s_d can relevantly reduce the drying of façades. S_MW and S5 are the systems that work best for the drying of walls in Lisbon and Porto, at least in the first 4 years of drying. This result is coherent with the low s_d of the systems, which is below 0.5 m, together with their good ability to reduce rainwater intake. Also for the walls in Bologna, S5 and S_MW appear to work well, at least after the first year of drying, providing for similar results to the original render. In these walls, where the substrate has high capillary water absorption coefficient and free water saturation, S_MW gives slower drying than S5 in the beginning of the drying process. This result suggests that in the first phase of drying, when liquid
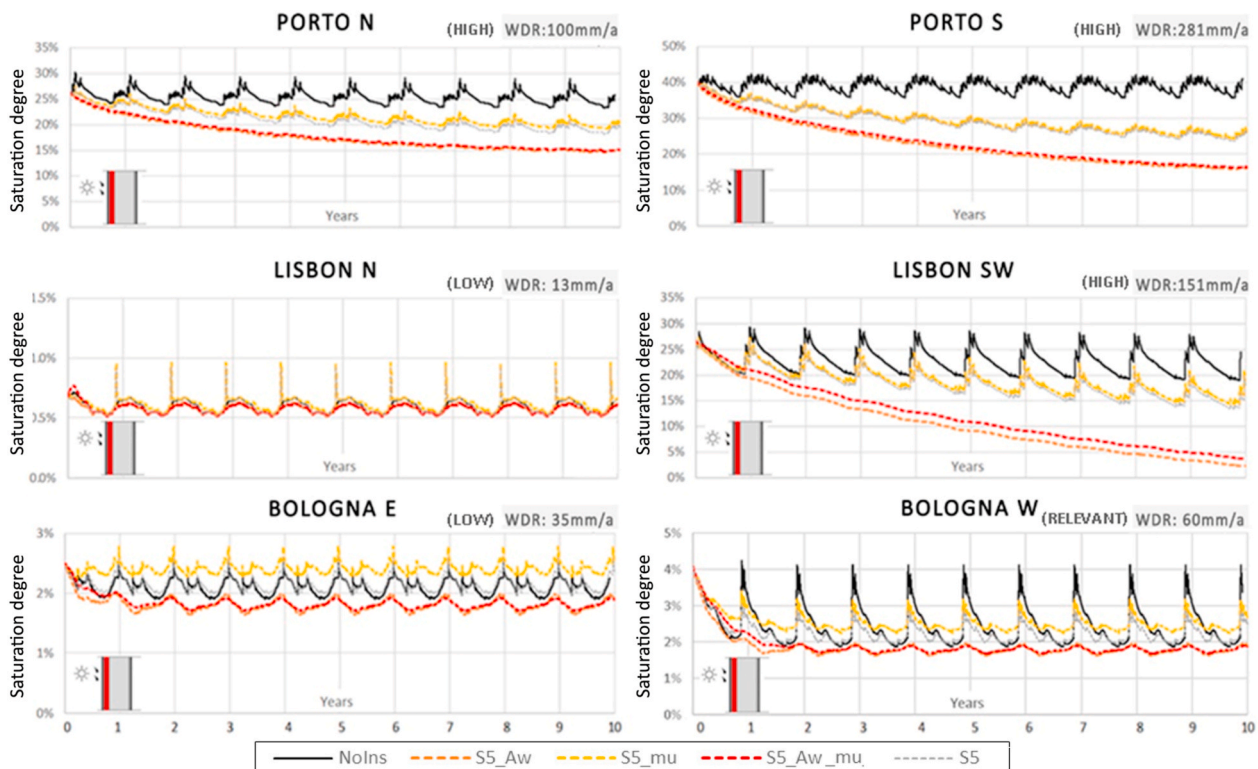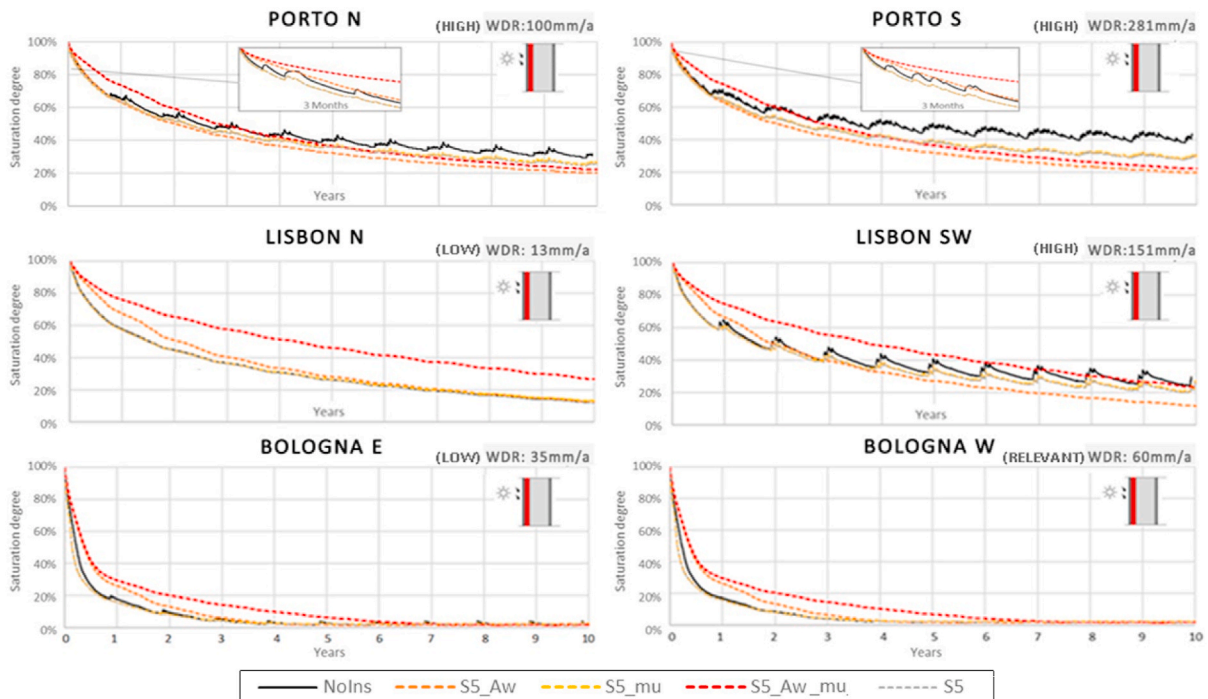

Fig. 15. Saturation degree in walls substrate in the original and retrofitted scenarios(parametric study on external insulation).

transport is more relevant than the drying through vapour diffusion, a capillary active insulation material can perform better than a hydrophobic one, for systems that have a comparable s_d. Systems S2 and S4, noticeably reduce the drying of walls in Lisbon and Bologna, in the second to fourth year of drying, in comparison to the original configuration. This seems the effect of the poor balance of the systems in terms of drying and rainwater intake. This behaviour appears to have a

noticeable effect on walls having a quite capillary-active substrate, such as in Lisbon and Bologna, while it does not appear significant in the granite walls of Porto.

In Fig. 17 the saturation degree observed in the parametric study on hygric properties, during drying, is presented.

The worst performance among the retrofitted scenarios is observed with the system that has both a high s_d and a low A_w (S5_Aw_mu), at
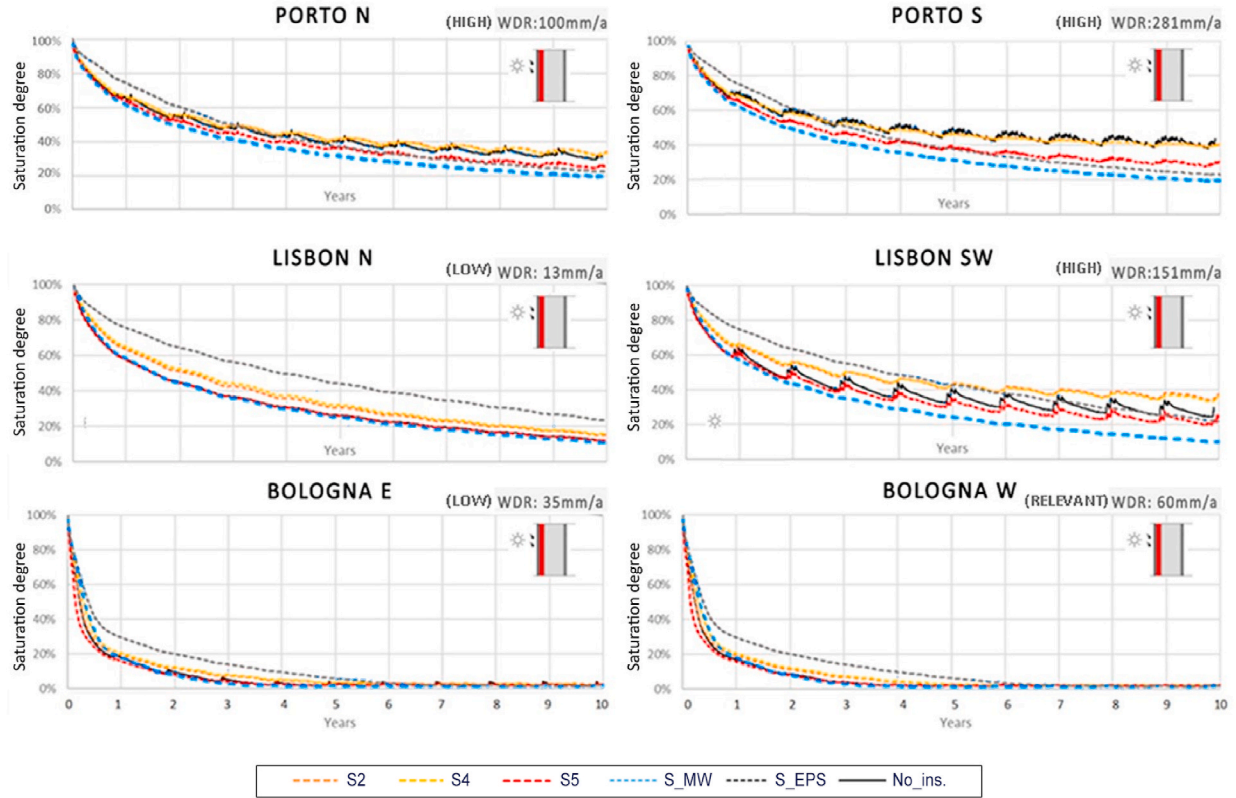
Fig. 16. Saturation degree in walls substrate during drying from saturation, in the original and retrofitted scenarios (external insulation).

Fig. 17. Saturation degree in walls substrate during drying from saturation, in the original and retrofitted scenarios (parametric study on external insulation).

least in the first 4 years of drying, similarly to what was previously observed with S_EPS. S5_A$_w$ reduces the drying of the walls in Lisbon and Bologna much more relevantly than S5, at least in the first 2 years of drying. This outcome seems to be the result of the reduced liquid transport to the external surface of the wall, where the drying from the moist surface happens, which appears significant for limestone and brick walls, i.e. the ones having relevant capillary activity. In Porto, where walls have a low capillary absorption coefficient, this effect is observable for a much shorter period, namely for a few months after the intervention, as shown in the detail of the first 3 months of drying. In all cases, S5_mu does not appear to reduce the drying of the walls, in comparison to S5. This can be explained by the fact that the insulation layer considered is capillary active, so the water is taken from the thermal mortar to the coating mortar by liquid transport, and from there liquid and vapour transport can occur thanks to the low s$_d$ of the coating mortar. With a hydrophobic and vapour proof finishing the result might be quite different and the drying much reduced. By contrast, when the insulation has a high s$_d$ in combination with a low A$_w$, the drying slows down relevantly more than with S5_A$_w$. This result indicates that when drying via liquid transport is reduced, the vapour permeability of the insulation gets very relevant, being then vapour diffusion the main moisture transport mechanism.

Overall, the worse drying is observed with a system having high s$_d$ (s$_d$ > 2 m), and the best results are obtained with systems having s$_d$ < 0.5 m, while being below the German curve for stuccos and coatings. One exception is observed, namely with S5_A$_w$. This system has low A$_w$ and s$_d$, complying with the strict EAD requirements. Nonetheless, it appears to relevantly slow down the drying of four walls, in the first years. This outcome seems to be the result of the hydrophobic nature of the insulation layer, which reduces moisture transport in the first phase of drying, together with a vapour permeability that is not sufficiently low to compensate for this drawback, as opposed to S_MW. Anyway, this behaviour is relevant only in the first 2–3 years of drying, when saturation degree is very high, and it is not relevant in low capillary-active walls such as the ones made of granite, i.e. those in Porto.

Overall, systems that do not comply with the maximum s$_d$ of 2 m, appear to have potentially detrimental effects on the drying of the walls. Furthermore, it is interesting to underline that those solutions that

comply with the German hyperbola but not with the maximum s$_d$ of 2 m, such as S_EPS, can show very good performance under operational conditions but very negative ones during drying from saturation.

8. Synthesis of results

The results obtained in this study are synthesized in a matrix of risk, which is reported in Table 4.

At the top of the table, the walls considered are reported, which are organized according to a climatic parameter, namely the ratio WDR/solar radiation. This parameter is adopted to account for the fact that a higher load of rain leads to higher moisture content while higher solar radiation theoretically reduces it through an increased drying. Thus, from left to right the walls exposed to extremer to milder outdoor climatic conditions are reported. The first three walls are the ones exposed to high WDR, followed by those exposed to relevant and low WDR. In the same table, the thermal insulation systems are ordered according to their s$_d$*A$_w$. This parameter is considered due to its relevance for moisture accumulation in the walls. To help synthesize the results, the s$_d$ values of the insulation systems are also reported in the table and represented in bold when exceeding 2 m. Similarly, the s$_d$*A$_w$>0.2 kg m^{-1} h$^{-0.5}$ are indicated in bold, and solutions that do not exceed these two limitations are underlined.

Some observations can be drawn from the matrix of risks:

- The highest reduction of water content can be obtained in walls exposed to high WDR. This outcome is clearly the result of the reduction of rainwater intake provided by some of the systems.
- Best performances are observed with systems having a very low A$_w$*s$_d$, namely those complying with the EAD recommendations (A$_w$ ≤ 0.10 kg m^{-2} h$^{-0.5}$, s$_d$ ≤ 1 m) i.e., S5_A$_w$ and S_MW. This outcome indicates that systems having low capillary water absorption and high vapour permeability appear more hygric-compatible than other solutions, for external interventions on traditionally constructed masonry walls.
- Thermal mortar-based system S5, which exceeds EAD recommendations but complies with the German requirements on A$_w$*s$_d$ and maximum A$_w$ and s$_d$, provides good performance. Indeed, it leads to

Table 4
Indexes of risk with external insulation (moisture content in the wall substrate and drying from saturation).

Wall:			PORTO S	PORTO N	LISBON SW	BOLOGNA W	BOLOGNA E	LISBON N
Climatic parameter (WDR/solar radiation):			0.31	0.28	0.13	0.06	0.06	0.03
s$_d$	(S$_d$*A$_w$)	SYSTEM	Moisture accumulation in the substrate (from regular initial water content) – risk indexes					
0.08	0	S_MW	-40%	-24%	-27%	-27%	-15%	-4%
0.39	0.02	S5_Aw	-39%	-23%	-25%	-26%	-14%	-4%
2.03	0.11	S5_A_mu	-29%	-14%	-18%	-19%	-12%	-4%
2.03	0.11	S_EPS	-30%	-16%	-18%	-20%	-13%	-4%
0.39	0.13	S5	-36%	-21%	-9%	-9%	2%	0%
0.94	**0.28**	S4	-34%	-19%	4%	14%	8%	3%
0.83	**0.4**	S2	-34%	-19%	10%	22%	11%	7%
2.03	**0.66**	S5_mu	-36%	-21%	-8%	4%	14%	3%
S$_d$	(S$_d$*A$_w$)	SYSTEM	Drying from saturation – risk indexes					
0.08	0	S_MW	-13%	-13%	-7%	-14%	-8%	-1%
0.39	0.02	S5_Aw	-11%	-11%	6%	47%	56%	14%
2.03	0.11	S5_A_mu	21%	21%	42%	140%	147%	44%
2.03	0.11	S_EPS	8%	8%	36%	121%	131%	44%
0.39	0.13	S5	-6%	-6%	-1%	-10%	-8%	-1%
0.94	**0.28**	S4	3%	3%	17%	38%	40%	17%
0.83	**0.4**	S2	3%	3%	15%	28%	30%	14%
2.03	**0.66**	S5_mu	-5%	-5%	-1%	-7%	-5%	-1%
Risk assessment – ranking scales:								
			High risk	Low risk	Neutral	Low benefit	High benefit
Moisture accumulation			22% ÷ 11%	11% ÷ 0%	0%	0% ÷ -20%	-20% ÷ -40%
Reduction of Drying			147% ÷ 74%	74% ÷ 0%	0%	0% ÷ -7%	-7% ÷ -14%

Notation: Climatic parameter: annual sum of WDR [mm/a] divided by the annual solar radiation [kWh/m²a]; s$_d$: equivalent-air-thickness [m], A$_w$: capillary water absorption coefficient [kg/ (m² h)].

benefits or very low risks in terms of moisture content in the walls. Additionally, it provides moderate benefits with regard to the drying of the walls.

- Systems that comply with the German hyperbola but exceed the maximum s_d, namely S_EPS and S5_A_w_mu, appear very risky. Indeed, although showing good performance under typical operational conditions, they have detrimental effects on drying from saturation.
- Finally, systems exceeding the hyperbola $(A_w*s_d) = 0.2$ kg m^{-1} h$^{-0.5}$, namely S2, S4, and S5_mu, show bad performance. In fact, they are the only solutions leading to a high risk of moisture accumulation.

9. Conclusion

A common guideline for choosing hygric-compatible insulation solutions for historic and traditional walls is not yet available. Nonetheless, it seems possible to define recommendations for specific clusters of interventions. This study addressed the cluster of thermal rendering systems for traditional and historic masonry walls, in bricks or stone, located in temperate climates with mild winter conditions. The recommendations defined in the study can be summarized as follows:

- The impact of external thermal rendering systems on the water content of walls depends on the effect they have on the wetting and drying of the components, as observed in the German standard DIN 4108–3:2018 for rain protective stuccos and coatings.
- This impact depends on the hygric properties of thermal rendering systems (measured for the composite layered system as a complete unit): capillary water absorption, A_w, and equivalent air thickness, s_d.
- Vapour permeable thermal rendering systems with low capillary absorption coefficients, such as system S5, appear suitable for the intervention. More in detail, solutions complying with the restrictions $A_w*s_d < 0.2$ kg m^{-1} h$^{-0.5}$, $s_d < 2$ m and $A_w \leq 0.5$ kg m^{-2} h$^{-0.5}$ are recommended for the sake of guaranteeing hygric compatibility. Solutions complying with the stricter indications $A_w < 0.10$ kg/(m^2.h$^{0.5}$) and $s_d < 1$ m, are further preferable.
- The recommendations provided in the previous point refer to the choice of thermal rendering systems, in the early stage of design. When intervening on valuable walls, further investigations should be performed to confirm the hygric compatibility of the design, while considering the specific boundary conditions and materials involved in the scenario under analysis.

Finally, this study allowed to compare the performance of thermal rendering systems to solutions based on more common insulation materials, such as Expanded Polystirene and Hydrophobic mineral wool. Results show that for all types of insulation materials it is important to simulate the hygrothermal behaviour of walls starting from very moist conditions in the substrate, such as close to saturation. Indeed, some drawbacks might be overlooked if only typical moisture content and operational conditions are considered. For instance, solutions with a $s_d > 2$ m and a hydrophobic insulation layer can perform well under typical operational conditions, but they have detrimental effects on the drying of walls from saturation. Thus, the use of these solutions, such as those relying on an insulation layer of EPS, should be discouraged in historic and

traditional walls. These walls are typically made of porous materials and have no capillary breaks, thus high moisture levels may occur in some parts of the construction, due to damages in the envelope, pipe leakage, rising damp or even floods. In these areas, solutions that reduce the drying ability of walls may lead to trapped moisture and increased rising damp, with the degradation risks and increased heat losses that those entail.

It is worth underlining that the outcomes of this paper are based on validated hygrothermal simulations, and that future experimental studies should be devoted to corroborate the recommendations hereby presented.

ANNEX I. COMPLEMENTARY SIMULATIONS: Moisture accumulation in Lisbon walls when different coatings are adopted for thermal rendering systems

In the study, the hygrothermal behaviour of massive walls retrofitted with various external thermal insulation solutions was evaluated. Good performances were observed with system S5 and poor ones with systems S2 and S4, especially in the walls located in Lisbon. The latter two systems resulted in moisture accumulation in the SW-oriented wall in Lisbon.

The different behaviour of the external insulation systems is considered to be strongly dependent on the coating adopted in the insulation system. This assumption is hereby investigated with some complementary simulations. The three thermal mortars A1, A2, and A3 are adopted with different

coatings, namely B1+C2 and B2. The A_w and s_d of the systems are synthesized in Fig. I.1. All systems finished with B2, i.e. S5, A1+B2, and A2+B2, fall inside the hyperbola $A_w*s_d = 0.2$ kg m^{-1} h$^{-0.5}$, whereas all systems finished with B1+C2 (i.e., S2, S4 and A3+B1+C2) exceed this limit.
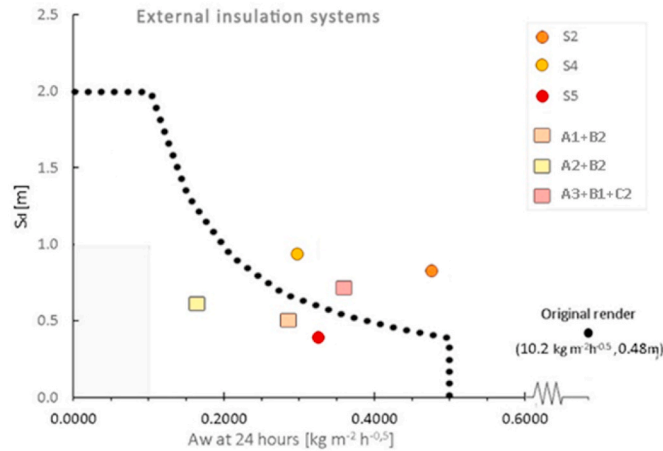

Fig. I.1. – Equivalent air layer thickness (s_d) and capillary absorption coefficient (Aw) of external insulation systems and original render. Study on different coating for thermal mortar-based insulation systems: S2 (A1+B1+C2), S4 (A2+B1+C2), S5 (A3+B2), A1+B2, A2+B2, and A3+B1+C2.

Results obtained in terms of moisture content under operational conditions are reported in Fig. I.2. All thermal mortars do not lead to relevant moisture increase when covered with mortar B2. On the contrary, they lead to a noticeable increase (and even accumulation in the SW-oriented wall) when finished with B1+C2. Thus, coating B1+C2 seems a risky choice. The results obtained further confirm that the use of rendering systems exceeding the recommended hyperbola should be avoided.
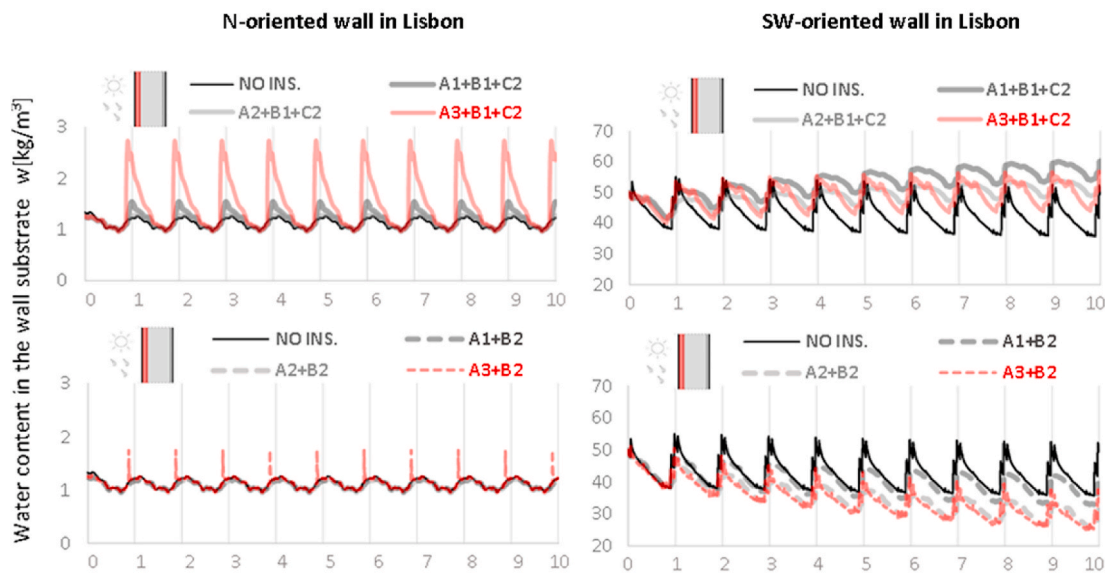

Fig. I.2. Water content in the wall substrate of the original and retrofitted walls in Lisbon. Thermal rendering systems which adopt B1+C2 and B2 are shown in the top and bottom graphics, respectively.

References

[1] A. Galimshina, et al., Statistical method to identify robust building renovation choices for environmental and economic performance, Build. Environ. 183 (2020), https://doi.org/10.1016/j.buildenv.2020.107143.

[2] V. Göswein, J. Reichmann, G. Habert, F. Pittau, Land availability in Europe for a radical shift toward bio-based construction, Sustain. Cities Soc. 70 (2021), https://doi.org/10.1016/j.scs.2021.102929.

[3] E. Cintura, P. Faria, M. Duarte, L. Nunes, Bio-wastes as aggregates for eco-efficient boards and panels: screening tests of physical properties and bio-susceptibility, Infrastructure 7 (3) (2022), https://doi.org/10.3390/infrastructures7030026.

[4] K. Kompatscher, R.P. Kramer, B. Ankersmit, H.L. Schellen, Intermittent conditioning of library archives: microclimate analysis and energy impact, Build. Environ. (2019), https://doi.org/10.1016/j.buildenv.2018.10.013.

[5] A. Egusquiza et al., "Co-creation of local eco-rehabilitation strategies for energy improvement of historic urban areas," Renew. Sustain. Energy Rev., vol. 135, 2021, doi: 10.1016/j.rser.2020.110332.

[6] H.M. Künzel, Effect of interior and exterior insulation on the hygrothermal behaviour of exposed walls, Mater. Struct. Constr. (1998), https://doi.org/10.1007/bf02486471.

[7] S. Doran, G. Zapata, C. Tweed, C. Suffolk, T. Forman, A. Gemmell, Solid wall heat losses and the potential for energy saving, BRE Rep. Dep. Energy Clim. Chang. 44 (2014), 0.

[8] M. Amorim, V.P. Freitas, I. Torres, T. Kisilewicz, U. Berardi, The Influence of Moisture on the Energy Performance of Retrofitted Walls, MATEC Web Conf., 2020, https://doi.org/10.1051/matecconf/202032201035.

[9] Y. Govaerts, et al., Performance of a lime-based insulating render for heritage buildings, Construct. Build. Mater. 159 (2018) 376–389, https://doi.org/10.1016/j.conbuildmat.2017.10.115.

[10] D. Pickles, I. Brocklebank, C. Wood, Energy efficiency and historic buildings: application of Part L of the building regulations to historic and traditional constructed buildings, Energy Effic. Hist. Build. Appl. Part L Build. Regul. to Hist. Tradit. Constr. Build (2012) 1–72. November, 978-1-4098-3413-7.

[11] UNESCO, CONVENTION CONCERNING THE PROTECTION OF THE WORLD CULTURAL AND NATURAL HERITAGE, 1972, 1972.

[12] M. Posani, R. Veiga, V.P. Freitas, Retrofitting historic walls: feasibility of thermal insulation and suitability of thermal mortars, Heritage 4 (3) (2021) 2009–2022, https://doi.org/10.3390/heritage4030114.

[13] M. Ibrahim, P.H. Biwole, P. Achard, E. Wurtz, G. Ansart, Building envelope with a new aerogel-based insulating rendering: experimental and numerical study, cost analysis, and thickness optimization, Appl. Energy 159 (2015), https://doi.org/10.1016/j.apenergy.2015.08.090.

[14] S. Malanho, R. Veiga, C.B. Farinha, Global performance of sustainable thermal insulating systems with cork for building facades, Buildings 11 (3) (2021), https://doi.org/10.3390/buildings11030083.

[15] J. L. Parracha et al., "Effects of hygrothermal, UV and SO2 accelerated ageing on the durability of ETICS in urban environments," Build. Environ., vol. 204, 2021, doi: 10.1016/j.buildenv.2021.108151.

[16] J. Maia, N.M.M. Ramos, R. Veiga, Evaluation of the hygrothermal properties of thermal rendering systems, Build. Environ. (2018), https://doi.org/10.1016/j.buildenv.2018.08.055.

[17] A. Henry, J. Stewart, Practical Building Conservation: Mortars, Renders & Plasters, 2011 in *English Heritage*.

[18] J. Maia, N.M.M. Ramos, R. Veiga, A new durability assessment methodology of thermal mortars applied in multilayer rendering systems, Construct. Build. Mater. 222 (2019), https://doi.org/10.1016/j.conbuildmat.2019.06.178.

[19] Cen, EN 998-1:2017 - 'Specification for Mortar for Masonry - Part 1: Rendering and Plastering Mortar, 2017.

[20] A. Ranesi, P. Faria, R. Veiga, "Traditional and Modern Plasters for Built Heritage: Suitability and Contribution for Passive Relative Humidity Regulation," Heritage, vol. 4, 2021, https://doi.org/10.3390/heritage4030132, 3.

[21] P. Maurenbrecher, Rilem TC 203-RHM: repair mortars for historic masonry: requirements for repointing mortars for historic masonry, Mater. Struct. 45 (2012) 1303–1309.

[22] R. Veiga, A. Fragata, A.L. Velosa, A.C. Magalhães, G. Margalha, Lime-based mortars: viability for use as substitution renders in historical buildings, Int. J. Architect. Herit. (2010), https://doi.org/10.1080/15583050902914678.

[23] J. Válek, J.J. Hughes, F. Pique, D. Gulotta, R. van Hees, I. Papayiani, Recommendation of RILEM TC 243-SGM: functional requirements for surface repair mortars for historic buildings, Mater. Struct. Constr. 52 (1) (2019), https://doi.org/10.1617/s11527-018-1284-y.

[24] I. Papayianni, V. Pachta, M. Stefanidou, Analysis of ancient mortars and design of compatible repair mortars: the case study of Odeion of the archaeological site of Dion, Construct. Build. Mater. 40 (2013), https://doi.org/10.1016/j.conbuildmat.2012.09.086.

[25] M. Posani, R. Veiga, V.P. Freitas, Towards resilience and sustainability for historic buildings: a review of envelope retrofit possibilities and a discussion on hygric compatibility of thermal insulations, Int. J. Architect. Herit. (2019), https://doi.org/10.1080/15583058.2019.1650132.

[26] D.S. Castele, A.L. Webb, Insulating the walls of historic buildings, APT Bull. J. Preserv. Technol. 50 (1) (2019) 37–44.

[27] I. McCaig, R. Pender, D. Pickles, "Energy Efficiency and Historic Buildings. How to Improve Energy Efficiency," Historic England, 2018.

[28] W. Anderson, J. Robinson, A Guide to Improving the Energy Efficiency of Traditional Homes in the City of Bath, Centre for Sustainable Energy, 2011.

[29] C. Wood, I. Brocklebank, D. Pickles, "ENERGY EFFICIENCY and HISTORIC BUILDINGS. Application of Part L of the Building Regulations to Historic and Traditionally Constructed Buildings," English Heritage, 2010.

[30] D. Pickles, I. McCaig, "EEHB - Energy Efficiency and Historic Buildings," Historic England, 2017.

[31] A. Richards, P. Smith, Improving Energy Efficiency in Historic Cornish Buildings, Cornwall Council Historic Environment Service, 2014.

[32] S. Zimmerman, Energy Costs in an Old House: Balancing Preservation and Energy Efficiency, vol. 2, Historic New England, Boston, 2008.

[33] J.E. Hensley, A. Aguilar, Preservation Brief 3: Improving Energy Efficiency in Historic Buildings, Technical Preservation Services, Washington, D.C., 2011.

[34] Effesus Project, Available online: http://www.effesus.eu/, 2016. (Accessed 11 February 2019).

[35] N.R.M. Sakiyama, J. Frick, H. Garrecht, Cultural heritage compatible insulation plaster: analysis and assessment by hygrothermal simulations, in: The 3rd International Conference on Energy Efficiency in Historic Buildings (EEHB2018), Visby, Sweden, 2018.

[36] T. Stahl, K. Ghazi Wakili, S. Hartmeier, E. Franov, W. Niederberger, M. Zimmermann, Temperature and moisture evolution beneath an aerogel based rendering applied to a historic building, J. Build. Eng. (2017), https://doi.org/10.1016/j.jobe.2017.05.016.

[37] T. Stahl, S. Brunner, M. Zimmermann, K. Ghazi Wakili, Thermo-hygric properties of a newly developed aerogel based insulation rendering for both exterior and interior applications, Energy Build. 44 (1) (2012) 114–117, https://doi.org/10.1016/j.enbuild.2011.09.041.

[38] M. Posani, R. Veiga, and V. P. Freitas, "Thermal mortar-based insulation solutions for historic walls: an extensive hygrothermal characterization of materials and systems," Construct. Build. Mater., vol. 315, 2022, doi: 10.1016/j.conbuildmat.2021.125640.

[39] Din, DIN 4108-3 Thermal Protection and Energy Economy in Buildings - Part 3: Protection against Moisture Subject to Climate Conditions - Requirements, Calculation Methods and Directions for Planning and Construction, 2018.

[40] Eota, ETAG 004:2013 - "Guideline for European Technical Approval of External Thermal Insulation Composite Systems (ETICS) with Rendering, 2013.

[41] E. Lucchi, et al., Development of a compatible, low cost and high accurate conservation remote sensing technology for the hygrothermal assessment of historic walls, Electron 8 (6) (2019), https://doi.org/10.3390/electronics8060643.

[42] M. Andreotti, M. Calzolari, P. Davoli, L.D. Pereira, E. Lucchi, R. Malaguti, Design and construction of a new metering hot box for the in situ hygrothermal measurement in dynamic conditions of historic masonries, Energies 13 (11) (2020), https://doi.org/10.3390/en13112950.

[43] M. Andreotti, et al., Applied Research of the hygrothermal behaviour of an internally insulated historicwall without vapour barrier: in situ measurements and dynamic simulations, Energies 13 (13) (2020), https://doi.org/10.3390/en13133362.

[44] B. Tejedor, E. Lucchi, D. Bienvenido-Huertas, I. Nardi, Non-destructive techniques (NDT) for the diagnosis of heritage buildings: traditional procedures and futures perspectives, Energy Build. 263 (2022), https://doi.org/10.1016/j.enbuild.2022.112029.

[45] G. Ficco, F. Iannetta, E. Ianniello, F.R. D'Ambrosio Alfano, M. Dell'Isola, U-value in situ measurement for energy diagnosis of existing buildings, Energy Build. 104 (2015), https://doi.org/10.1016/j.enbuild.2015.06.071.

[46] B. Andra, E.J. de P. Hansen, et al., RIBuild (Robust Internal Thermal Insulation of Historic Buildings, EU Project) - written guidelines for decision making concerning the possible use of internal insulation in historic buildings (Deliverable no. D6.2) [Online]. Available: https://www.ribuild.eu/s/Written-guidelines-for-decision-making-concerning-the-possible.pdf, 2020.

[47] D. Zirkelbach, T. Schmidt, M. Kehrer, H.M. Künzel, WUFI® Pro 5 manual [Online]. Available: https://wufi.de/download/WUFI-Pro-5_Manual.pdf%5Cnhttps://wufi.de/en/wp-content/uploads/sites/11/2014/09/WUFI-Pro-5_Manual.pdf, 2007.

[48] H.M. Künzel, Simultaneous Heat and Moisture Transport in Building Components One- and Two-Dimensional Calculation Using Simple Parameters, vol. 1995, 1995, ISBN 3-8167-4103-7.

[49] K. Martin, T.N.S. Klaus, Application of Software Tools for Moisture Protection of Buildings in Different Climate Zones Special Example: Control of Air Humidifier in a Cold Climate for High Comfort and No Risk of Mould Growth in Building Room, Heating, Vent. Air-Conditioning, Sisimiut, Groenl., 2009.

[50] A. Evrard, C. Flory-Celini, M. Claeys-Bruno, A. De Herde, Influence of liquid absorption coefficient on hygrothermal behaviour of an existing brick wall with Lime-Hemp plaster, Build. Environ. 79 (2014), https://doi.org/10.1016/j.buildenv.2014.04.031.

[51] P. Cabrera, H. Samuelson, M. Kurth, Simulating mold risks under future climate conditions, in: Building Simulation Conference Proceedings, vol. 3, 2019.

[52] O. Hägerstedt, J. Arfvidsson, Comparison of Field Measurements and Calculations of Relative Humidity and Temperature in Wood Framed Walls, 2010.

[53] B. Villmann, Time-dependent moisture distribution in drying cement mortars – results of neutron radiography and inverse analysis of drying tests, Restor. Build. Monum. (2014), https://doi.org/10.12900/rbm14.20.1-0004.

[54] S.O. Mundt-Petersen, L.E. Harderup, Validation of a One-Dimensional Transient Heat and Moisture Calculation Tool under Real Conditions, 2013.

[55] Ü. Alev, T. Kalamees, M. Teder, M.-J. Miljan, Air Leakage and Hygrothermal Performance of an Internally Insulated Log House, in: NSB 2014 10th Nord. Symp. Build. Phys., 2014.

[56] B. Stöckl, D. Zirkelbach, H.M. Künzel, Hygrothermal Simulation of Green Roofs-New Models and Practical Application, 2014.

[57] G.R. Finken, S.P. Bjarløv, R.H. Peuhkuri, Effect of façade impregnation on feasibility of capillary active thermal internal insulation for a historic dormitory - a hygrothermal simulation study, Construct. Build. Mater. 113 (2016) 202–214, https://doi.org/10.1016/j.conbuildmat.2016.03.019.

[58] A. Abdul Hamid, P. Wallentén, Hygrothermal assessment of internally added thermal insulation on external brick walls in Swedish multifamily buildings, Build. Environ. (2017), https://doi.org/10.1016/j.buildenv.2017.05.019.

[59] T. Stahl, K.G. Wakili, S. Hartmeier, E. Franov, W. Niederberger, M. Zimmermann, Temperature and moisture evolution beneath an aerogel based rendering applied to a historic building, J. Build. Eng. 12 (2017) 140–146.

[60] D. Kaczorek, Hygrothermal Assessment of Internally Insulated Brick Wall Based on Numerical Simulation, 2018, https://doi.org/10.1088/1757-899X/415/1/012013.

[61] I.M. Lisitano, et al., Energy in cultural heritage: The case study of monasterio de santa maria de monfero in galicia, 2018.

[62] S. Vacek, R. Kostelník, Case study of application of capillary active thermal insulation systems used as an interior insulation for historical buildings, in: Proceedings of the International Conference of Buildings and Environments, 2019, https://doi.org/10.2478/9788395669699-034.

[63] E. Barreira, M.L. Simões, J.M.P.Q. Delgado, I. Sousa, Procedures in the construction of a test reference year for Porto-Portugal and implications for hygrothermal simulation, Sustain. Cities Soc. 32 (2017) 397–410, https://doi.org/10.1016/j.scs.2017.04.013. December 2016.

[64] METEOTEST Meteonorm - VErsion 6.0. Meteotest, Bern, Switzerland.

[65] B. Blocken, J. Carmeliet, A review of wind-driven rain research in building science, J. Wind Eng. Ind. Aerod. 92 (13) (2004), https://doi.org/10.1016/j.jweia.2004.06.003.

[66] M.L.M. Nascimento, E. Bauer, J.S. de Souza, V.A.G. Zanoni, Wind-driven rain incidence parameters obtained by hygrothermal simulation, J. Build. Pathol. Rehabil. (2016), https://doi.org/10.1007/s41024-016-0006-5.

[67] Fraunhofer-Institut für Bauphysik, WUFI Pro 5 - Materials Database, 2007.

[68] M.I.M. Torres, V.P. Freitas, Treatment of rising damp in historical buildings: wall base ventilation, Build. Environ. (2007), https://doi.org/10.1016/j.buildenv.2005.07.034.

[69] C.S.F.M. Ferreira, Inércia higroscópica em museus instalados em edifícios antigos - Utilização de técnicas passivas no controlo da humidade relativa interior, FEUP, 2015.

[70] R. Veiga, A. Fragata, A.L. Velosa, A.C. Magalhães, G. Margalha, Lime-based mortars: viability for use as substitution renders in historical buildings, Int. J. Architect. Herit. (2010), https://doi.org/10.1080/15583050902914678.

[71] A.L. Damas, R. Veiga, P. Faria, Caraterização de argamassas antigas de Portugal – contributo para a sua correta conservação, in: Congresso Ibero-Americano "Património, suas Matérias e Imatérias, 2016.

[72] A.L. Velosa, R. Veiga, Argamassas do Património Histórico: conhecer para conservar e reabilitar, in: Congresso internacional sobre patologia e reabilitação de estruturas, vol. 12, 2016.

[73] C.A.P. Santos, J.A.V. Paiva, Coeficientes de transmissão térmica de elementos da envolvente dos edifícios (ITE-54), LNEC, Lisbon, 2006.

[74] P.F.G. Banfill, Hygrothermal simulation of building performance: data for Scottish masonry materials, Mater. Struct. Constr. 54 (4) (2021), https://doi.org/10.1617/s11527-021-01759-x.

[75] E. Lucchi, Thermal transmittance of historical brick masonries: a comparison among standard data, analytical calculation procedures, and in situ heat flow meter measurements, Energy Build. (2017), https://doi.org/10.1016/j.enbuild.2016.10.045.

[76] J. Grunewald, U. Ruisinger, P. Häupl, The Rijksmuseum Amsterdam - hygrothermal analysis and dimensioning of thermal insulation, in: 3rd International Building Physics, Montreal, Quebec, Canada, 2006.

[77] W.L. Oberkampf, C.J. Roy, Verification and Validation in Scientific Computing, Cambridge University Press, 2010.

[78] S.O. Mundt-Petersen, L.-E. Harderup, A method for blind validation of hygrothermal calculation tools, in: Proceedings XIII DBMC–XIII International Conference on Durability of Building Materials and Components, 2014, pp. 624–631.

[79] I. Costa-Carrapiço, B. Croxford, R. Raslan, J.N. González, Hygrothermal calibration and validation of vernacular dwellings: a genetic algorithm-based optimisation methodology, J. Build. Eng. (2022), 104717.

[80] ASHRAE, Measurement of energy and demand savings, ASHARE Guidel 14–2002 (2002).

[81] K. Kompatscher, R.P. Kramer, B. Ankersmit, H.L. Schellen, Intermittent conditioning of library archives: microclimate analysis and energy impact, Build. Environ. 147 (2019) 50–66, https://doi.org/10.1016/j.buildenv.2018.10.013.

[82] M. Posani, R. Veiga, V.P. Freitas, K. Kompatscher, H. Schellen, Dynamic hygrothermal models for monumental, historic buildings with HVAC systems: complexity shown through a case study, E3S Web of Conferences 172 (2020), 15007.

[83] M. Giuliani, G.P. Henze, A.R. Florita, Modelling and calibration of a high-mass historic building for reducing the prebound effect in energy assessment, Energy Build. 116 (2016), https://doi.org/10.1016/j.enbuild.2016.01.034.

[84] A. Sadłowska-Sałęga, J. Radoń, Feasibility and limitation of calculative determination of hygrothermal conditions in historical buildings: case study of st. Martin church in Wiśniowa, Build. Environ. (2020), https://doi.org/10.1016/j.buildenv.2020.107361.

[85] G.B.A. Coelho, H.E. Silva, F.M.A. Henriques, Calibrated hygrothermal simulation models for historical buildings, Build. Environ. (2018), https://doi.org/10.1016/j.buildenv.2018.06.034.

[86] G.R. Ruiz, C.F. Bandera, Validation of calibrated energy models: common errors, Energies (2017), https://doi.org/10.3390/en10101587.

[87] M. Jerman, R. Černý, Effect of moisture content on heat and moisture transport and storage properties of thermal insulation materials, Energy Build. (2012), https://doi.org/10.1016/j.enbuild.2012.07.002.

[88] J.L. Parracha, et al., Performance parameters of ETICS: correlating water resistance, bio-susceptibility and surface properties, Construct. Build. Mater. (2021), https://doi.org/10.1016/j.conbuildmat.2020.121956.

[89] H.M. Künzel, H. Künzel, A. Holm, Rain protection of stucco facades, in: Proc. Therm. Perform. Exter. Envel. Whole Build. IX–International Conf. Florida, USA, 2004.

[90] J. Zhao, J. Grunewald, U. Ruisinger, S. Feng, Evaluation of capillary-active mineral insulation systems for interior retrofit solution, Build. Environ. 115 (2017) 215–227, https://doi.org/10.1016/j.buildenv.2017.01.004.

[91] T.S. Freitas, A.S. Guimarães, S. Roels, V.P. Freitas, A. Cataldo, Is the time-domain reflectometry (TDR) technique suitable for moisture content measurement in low-porosity building materials? Sustain. Times 12 (19) (2020) https://doi.org/10.3390/SU12197855.

[92] R. Veiga, Conservation of historic renders and plasters: from laboratory to site, RILEM Bookseries (2013), https://doi.org/10.1007/978-94-007-4635-0_16.

[93] E. Vereecken, L. Van Gelder, H. Janssen, S. Roels, Interior insulation for wall retrofitting–A probabilistic analysis of energy savings and hygrothermal risks, Energy Build. 89 (2015) 231–244.

[94] E. Vereecken, S. Roels, Capillary active interior insulation: do the advantages really offset potential disadvantages? Mater. Struct. 48 (9) (2015) 3009–3021.